TÉCNICO LISBOA

Design of a compact aerosol system for controlled biocontaminations

Emanuel Moreira Escórcio da Câmara Cunha

Thesis to obtain the Master of Science Degree in

Biological Engineering

Supervisor: Prof. Susana Isabel Pinheiro Cardoso de Freitas
Supervisor: Cap. Wilson David Talhão Antunes

Examination Committee

Chairperson: Prof. Gabriel António Amaro Monteiro
Supervisor: Prof. Susana Isabel Pinheiro Cardoso Freitas
Member of the Committee: Prof. Paulo Jorge Peixeiro de Freitas

July 2017

Acknowledgements

Saying "thanks" is easy. Typing the gratefulness is oh-so-not. So it might come out a bit incoherent, but I guess a bit more honest, in a way. So thank you to all the following.

The waitress that was always nice to me, whenever I pulled an all-nighter at McDonalds. The pints at Trobadores, a lot of years ago, that I drank so desperately when I was told I wouldn't be able to keep taking my degree. My old friends from the first year of college. My childhood friends that always kept the spark of our friendship alive. My RPG group, for showing and sharing with me one of my biggest passion in life, and the intimacy of my heart.

The "task force" that helped me through the final stage of the thesis. Débora, who made me feel at home in INESC. Rita, for the down-to-earth evaluations and project ambitions. Tomás Dias, for the assertiveness when addressing any point of this project, and valuable theoretical knowledge.

My whole family, away for years, that would love to be next to me in my presentation, but cannot. My father Luis, for being such an inspiration as a "future self", and having the right words at the right time to pull me back from my emotional drift. My mother Bela, the unstoppable force that always cared about the little well-being details of my life, even with me far away, and for unconsciously showing me why it is important to have a strong education, and persist for knowledge. My housemate, José Vieira, to which I cannot, in any way, show any kind of fair appreciation; a pillar to my adulthood, and a right arm during the age. My girlfriend's parents, Florença and Joaquim, for making me feel more than at home – within-family - in the weekends we spent together. My girlfriend Catarina: the angel from the sky, the warmth of my heart and the passion and adrenaline that fuels my waking up every day, for helping me during the hardship of the thesis delivery, and supporting me like I know she never supported anyone before.

My LBDB supervisor, Wilson Antunes, who made this thesis a pleasure, a true dream of investigation, something akin to my childhood dreams, while surely oblivious to it. My supervisor, Susana Cardoso Freitas, for having asked in that first TMN class if anyone wanted to do some slave work: a catapult to something I only dreamed of, the honor of saying I worked on my teenage dream, bionanotechnology; always with a friendly, welcoming and embracing word every time I sought a meeting, turning my anxiety in a joy that, to the day, I cannot express by words; you were a true inspiration as a scientist, and a person.

To my grandmother Bia. I know you would be proud to see me here.

To me: You stupid idiot, I told you I'd do it. You will not be the boss of me now. And never again.

To Mom and Dad,
for always believing in me
especially when I could not.

Abstract

With a steeping scientific development, and a knowledge so efficiently spread in the current century, any group can have access to previously restricted or confidential information. Such globalization brings a lot of beneficial progress, but on the other hand allows tools to be accessed by those that do not edify our society. And that's why it is the preventive capability that defines how good an organization reacts to what could be the unexpected.

The reappearing of attacks by rebel groups has created a need for knowing, controlling and neutralizing such threats. This investigation is therefore born: the design of a functional, simple and accessible system that can simulate with precision and exactness the dissemination of pathogenic microorganisms.

And if the design for an aerosolizer is something to be thought and created from scratch, its detection method is not. With the rise of biochips as the holy grail of bioassays, picking it was obvious. The portability, allied to a simple interface, good sensitivity and low investment make of it the go-to device to any kind of analysis that would by any other way, take much more time.

A system was therefore designed that could, not only simulate winds on a sample, through an air flux chamber, but also analyze and quantify the quantity of scattered microorganisms of said sample, by analysis of a platform composed of a cytometer, magnetoresistive sensors (spin valves), a microfluidic system, and an electronic unit for signal processing.

As a way of quantifying the contamination, *Bacillus thuringiensis* and *Bacillus cereus* spores, both species normally used as proxies for *Bacillus anthracis*, were prepared in liquid samples, simulating a sample withdrawn from the designed aerosol system, representing possible samples from both before and after the aerosolization.

The biology tests were conducted based on detections that were already established for other biological compounds. A significant difference was found between the control (53) and the positive sample (4316 peaks), therefore demonstrating the proof of concept.

Key words: Biocontamination, Lab-on-a-chip, Biosensor, Aerossolization, Pathogenic, Antrax, Simulation.

Resumo

Com um desenvolvimento científico cada vez mais acentuado, e a disseminação de informação tão eficiente neste século, qualquer grupo consegue ter acesso a informação outrora restrita ou confidencial. E se por um lado, essa globalização traz muitos progressos benéficos, por outro faz chegar ferramentas a quem com elas não edifica a nossa sociedade. Assim, cada vez mais, é a capacidade preventiva que define quão bem uma organização reage ao que poderia ser o imprevisto.

O ressurgir de ataques por parte de grupos rebeldes fez aparecer também uma necessidade de conhecer, e dentro do possível controlar e neutralizar essas ameaças. Nasce assim a ideia desta investigação: a criação de um sistema prático, simples e acessível, que consiga simular com precisão e exactidão a disseminação de microrganismos patogénicos.

E se o design de um aerossolizador é algo a ser pensado e criado de raiz, o método de detecção já não. Com o estabelecimento dos biochips como o santo graal da análise biológica, a sua escolha foi óbvia. A sua portabilidade, aliada a um interface simples, boa sensibilidade e baixo investimento fazem deles os dispositivos a recorrer para qualquer tipo de análise que, de outra forma, poderia ser relativamente demorada.

Concebeu-se então um sistema que permite, por um lado, simular ventos incididos sobre uma amostra, através de uma câmara de fluxo de ar, e por outro, analisar e quantificar a quantidade dispersa de microrganismos dessa mesma amostra, pela utilização de uma plataforma composta por um citómetro, sensores magnetoresistivos (*spin valves*), um sistema de microfluídica e uma unidade electrónica de processamento de sinal.

Como forma de quantificação da contaminação, esporos de *Bacillus thuringiensis* e *Bacillus cereus*, ambas espécies normalmente utilizadas como aproximação da espécie de *Bacillus anthracis*, foram assim preparadas em amostras líquidas, simulando uma recolha do sistema de aerosolização desenhado, representando possíveis amostras tanto prévias à aerossolização, como posteriores.

Os testes à biologia foram realizados com base em detecções que já se encontravam estabelecidas para outros compostos biológicos. Encontrou-se uma diferença significativa entre o negativo (53) e a amostra (4316 picos), demonstrando a prova de conceito.

Palavras-chave: Biocontaminação, Lab-on-a-chip, Biosensor, Aerossolização, Patogénico, Antrax, Simulação.

Contents

Figure Index

Abbreviation List

ADAM - Air Force Dispersion Assessment Model

DAC – Digital to analog converter

ELISA - Enzyme-linked immunosorbent assay

HEPA - High efficiency particulate air filter

IgG - Immunoglobulin G

INESC-MN - Instituto de Engenharia de Sistemas e Computadores – Microsistemas e Nanotecnologias

IPA - Isopropyl alcohol

LBDB - Laboratório de Bromatologia e Defesa Biológica

MP - Magnetic nanoparticles

nDies - Gold dies without antibodies, and with BSA instead (negative)

nMix - Solution of magnetic particles with no spores (negative)

nSample - Solution of magnetic particles with spores and BSA (negative)

PBS - Phosphate-buffered saline

pDies - Gold dies with antibodies (positive)

pMix - Solution of magnetic particles containing spores (positive)

pSample - Solution of magnetic particles with spores and antibodies (positive)

SV - Spin valve

Thesis structure

This thesis describes the design, for proof-of-concept, of both an aerosolization system, along with the protocol for a detection platform, to be used as a simulator and quantifier of airborne biocontaminations.

It should be noted that this work was the beginning of collaboration between Instituto de Engenharia de Sistemas e Computadores – Microsistemas e Nanotecnologias and the army's Laboratório de Bromatologia e Defesa Biológica, which ended up reinforcing the goal of the thesis as one of proof-of-concept. With that said, a number of options will be suggested throughout this work, but usually only one of the paths will be taken. For the same reason, special attention and emphasis was given to the detection part of the work, since it was the field the author was being directly and mostly evaluated over.

Chapter 1 refers to the motivations of this work, along with how the aerosolization of bacteria is usually executed and detected. Some notes are added on why this specific system should be developed.

Chapter 2 describes the full design of the aerosolization chamber. From schematics to the trajectory the particles take, the macro setup is revealed, and how all the variables can be manipulated and controlled.

Chapter 3 introduces the flow cytometry platform, going over the detection system. From the magnetoresistive spin valves that were created to the signal and noise that is read and filtered, each part of the working electronics is addressed. Some methods are included in this section, specifically for the electronics and components that the author did not directly produce.

Chapter 4 complements the platform explanation, but on the biological side. The microfluidics are explained, along with a description of the magnetic labelling, and reagent functionalization. Here, two methods will be shown and described: one using a sandwich ELISA test with surface functionalization, and another one using flow cytometry.

Chapter 5 reveals the methods chosen, and materials used. A detailed protocol of each and every step is included, so that this work can be reproduced, continued and complemented.

Chapter 6 shows the results achieved, and discusses what went wrong, what is to be avoided, and what should be tuned up to improve the process.

Chapter 7 is a general conclusion of this thesis, with a personal recommendation of what to address in future simulations, and pointing at new directions for the device as a whole.

1 Introduction

Natural sciences have always evolved alongside humanity, leaving its priceless contribution to our society. From Aristotle's work on species description and the natural philosophy model, and through Al-Farabi and Robert Kilwardby, soon the science revolution would start with the introduction of the modern scientific method, along with the differentiation of natural sciences into life sciences and physical sciences.

Development always comes at a price. A good example is the development of the V-2 missiles during the Second World War, a technology that came crucial for the engines of the space race, a few years later. Science can always harm as much as it can help.

While the physical sciences remain the true tool of warfare development, the recent rise in biological weapons brought a different approach to it, most notably by the 2001 anthrax attacks in the United States. The weaponization of bacteria goes back to the Nordic rebel poisoning of the Imperial Russian Army in 1916, but it was brought to the spotlight when a number of public institutions and workers received letters from an anonymous source containing as few as 5 grams of Bacillus anthracis spores (Figure 1, Figure 2). Even though it was later ruled out as a sociopath attack, it was first pointed out as a terrorist one, which started a completely new vision over the danger of weaponized biological species.

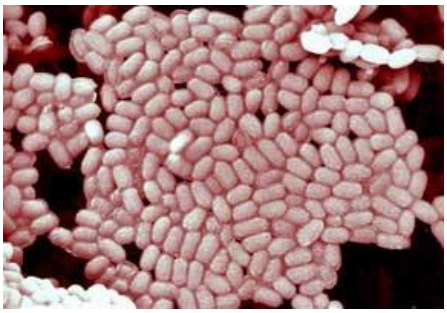

Figure 1 - Anthrax under magnification [Source: T. W. Geisbert / USAMRIID].

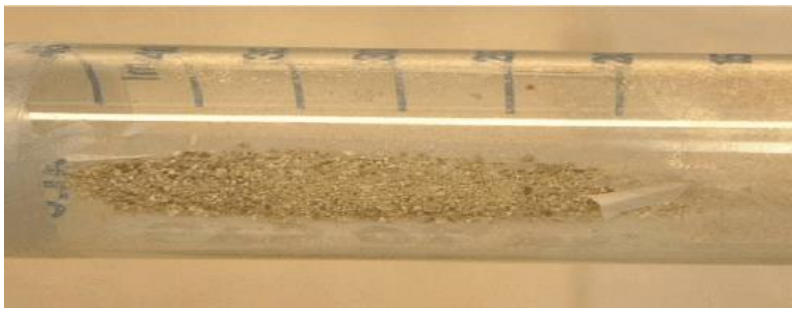

Figure 2 - New York Post letter powder [Source: FBI].

Almost invisible to the naked eye and of hard detection, but of extreme pathogenicity (Figure 3), these microorganisms have an incubation period of 7 days, with cutaneous infections fatal in 20% of the untreated cases (1% if treated), inhalations fatal in 75% of the cases even if treated, and intestinal infections fatal in 25% to 60% of the cases – the lethal dose being 10,000 spores[1]; it

is of extreme importance that these microorganisms are studied to know not only its effects, but also how they propagate, its speed of dissemination, behavior when airborne, and rate of aerosolization. But contrary to normal disease investigation, since this is a weaponized-base one, most of its research is made by the armed forces around the world.

Figure 3 - Lesions characteristic of cutaneous anthrax [Source: Biological weapons (2004)].

So how are these simulations done? Usually, either by software, or in very large aeration chambers. But in the beginning, on open military fields. A good example of such fields was the Dugway Proving Ground, a million acre land spread in the salt desert of Western Utah that served as testing station for agents and weapons since 1942 (Figure 4). Along with field and evaluation tests, Dugway conducts extensive research into ecology and epidemiology to register what happens to an area after many years of testing with lethal chemicals and highly infections bio agents[2]. Dugway ended up gaining notorious negative attention after a famous incident in 1968, known as the Skull Valley sheep kill, where allegedly a nozzle on an airplane spray malfunctioned, and released the infamous nerve agent VX over a huge flock of sheep. As a result, more than 6000 sheep were killed[3].

Figure 4 - Dugway Proving Grounds [Source: U.S. Army (2017)].

Nowadays, most of the simulations are made by computer, modeling aerosol dispersion in the case of intensive, small-scale convection by equalizing the concentration of anthrax spores over the building volume, predicting the time interval required for spore dispersion[4].

Very worth of mention is the Air Force Dispersion Assessment Model (ADAM), a program that simulates the atmospheric dispersion of several chemicals of interest to the U.S. Air Force[5]. With a graphical user interface, input/output file descriptions and reference to other readings on specific aspects of model calculations, it was released for public usage in December 11th, 1990. As we can see in Figure 5, ADAM allowed for a somewhat accurate estimation of the spread path, and would later calculate the time since release, distance from source, velocity of plume, and peak concentration.

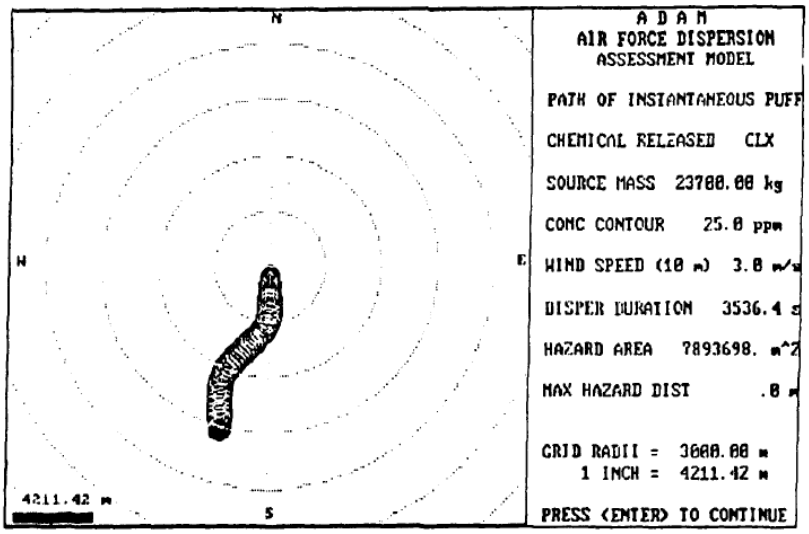

Figure 5 - Example of a simulation on ADAM [Source: ADAM user manual (1990)].

The need for an effective and realistic small scale simulator motivated most of what was developed in this work, although for now just on a proof-of-concept scale. And with so many obstacles to a safe study method, the usefulness of one more simulator was not even questioned.

2 Design

Even before any prototype, the design of the full aerosolizer changed a lot of times. From one obstacle or limitation to the other, all the aspects were reviewed, which ultimately was one of the main delays of this part of the project.

In the beginning, since the first idea was portability, all the pieces considered for it were chosen to be airtight, and high-grade steel. The idea was to design a two-part module system that could be easily assembled by bolting of the tubing border. The acceleration module would be the air entry, and would consist of either just a high efficiency particulate air (HEPA) filter, or have both an HEPA filter and the ventilating motor (Figure 6). A tube of low cross-section to channel the air against the sample was also being considered, so the high velocities could be reached.

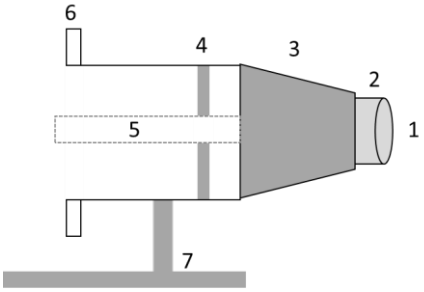

Figure 6 – Sketch for the acceleration module of the first system design. 1) Air entrance; 2) HEPA filter; 3) Entry cone; 4) Accelerating tube support; 5) Accelerating tube with an iris damper; 6) Bolting border; 7) System support.

This module would work attached to the aerosolization one (Figure 7), where a shelf would hold our sample, with an anemometer next to it, and one at the exit, to test how the velocity shifted. After the air exit, the sample collector would be attached to the system, allowing for the next step, the detection.

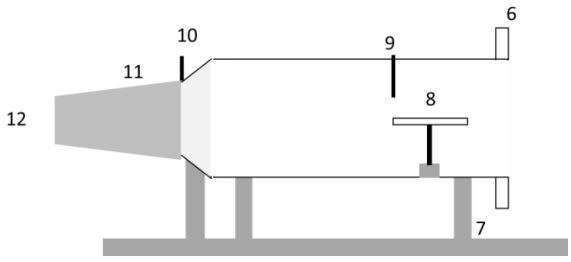

Figure 7 – Sketch for the aerosolization module of the first system design (numbered in continuation of Figure 6): 6) Bolting border; 7) System support; 8) Sample shelf; 9 and 10) Anemometer locations; 11) Exit cone with an iris damper; 12) Air exit.

The first full sketch of the system was therefore complete (Figure 8), and although nothing was defined as permanent, a starting point was set for discussion. The first thing that came into discussion was the amount of air flow needed for the velocity to be achieved. Even while taking into consideration a very small tube (7 cm), a flow of 77 l/s would have to be fed. This constrained our system in two ways: an HEPA filter to allow for such a large flow would have to be a compound filter, not just a membrane, thus dramatically increasing our system in size, and the sample collector had limiting flow (10x lower than what was needed).

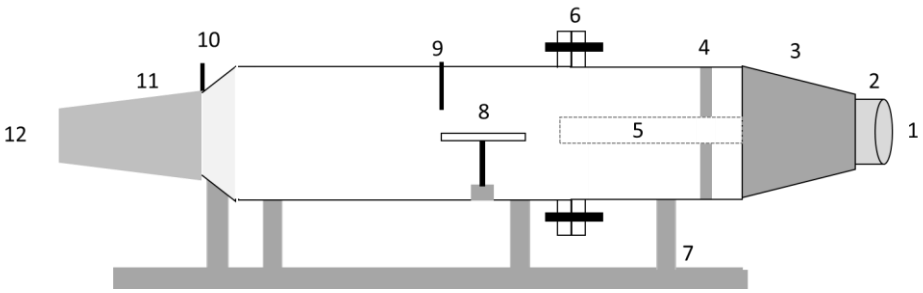

Figure 8 – Sketch for the acceleration module of the first system design. 1) Air entrance; 2) HEPA filter; 3) Entry cone; 4) Accelerating tube support; 5) Accelerating tube with an iris damper; 6) Bolting border; 7) System support; 8) Sample shelf; 9 and 10) Anemometer locations; 11) Exit cone with an iris damper; 12) Air exit.

A different approach was then studied, one that allowed for a more natural particle flow, and did not require an airtight chamber – by working on an existing isolated chamber, located at LBDB in Portela, Lisboa. The chamber schematics are shown in Figure 9.

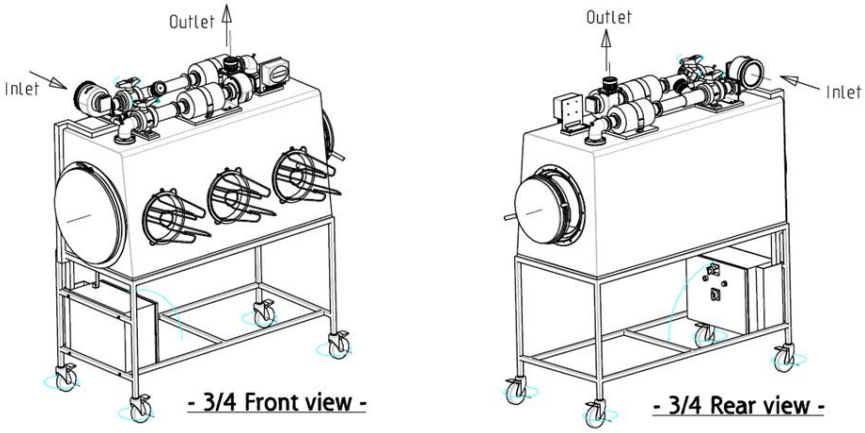

Figure 9 - Isolator GENTINGE La Calhène, with some custom built parts [Source: LBDB (2017)].

The assembling had to fit inside the isolated chamber, which raised some limitations: the width had to be lower than 0.35 m (to fit the circular entrance), the total length had to be inferior to 1 m, and all materials were required to be sterilizable. The chamber is supposed to be used with two different samplers, the SASSff 2300 wetted-wall air sampler[6] which extracts and transfers airborne pathogens, particulates, bacteria and spores from sampled air to small water volume for analysis (Figure 10), and the Sartorius™ MD8 Airport Portable Air Sampler[7], that uses a HEPA filter or a gelatin membrane filter method, guaranteeing reliable and exact measurement results (Figure 11).

Figure 10 - SASSff 2300 wetted-wall air sampler, and the cyclone unit inside that allows for the wetting of the solid particles contained in the aspirated air [Source: SASSff product website (2017)].

Figure 11 - Sartorius™ MD8 Airport Portable Air Sampler [Source: Sartorious™ product website (2017)].

Our new design had to be thought with some degree of mobility included, to allow for the relatively easy assembly inside the isolated chamber, and had to take into account that approximately 77 l/s had to be pushed through the main chamber, where the sample would be. Upon further discussion, it was decided that in order for the air flow to be as straight and unidirectional as possible, all obstacles had to be minimized: sudden walls or openings should be excluded, and the transitions between different diameters minimized. This lead to an increase in the air entrance diameter and to the transition from a sample chamber to a tube. The schematics for the full final aerosolizer are shown in Figure 12 and Figure 13:

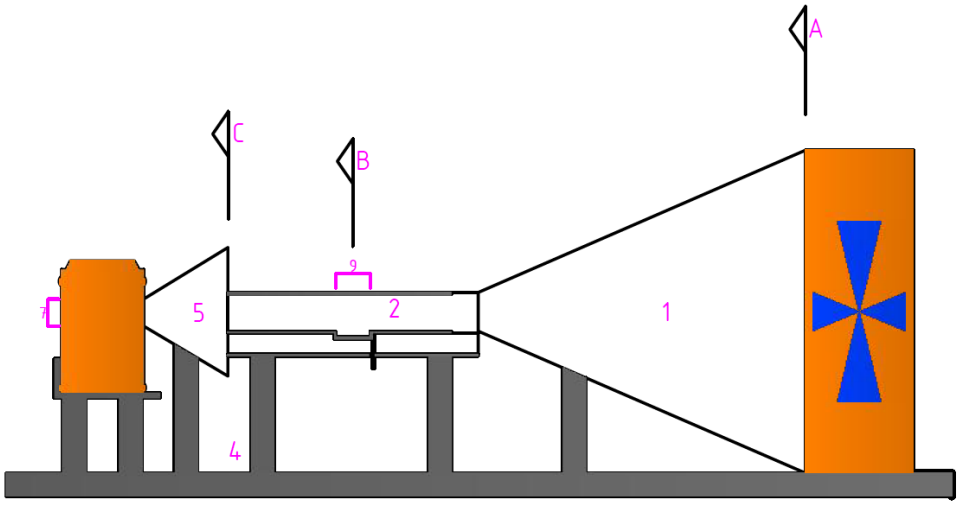

Figure 12 - Side view of the full aerosolization chamber, assembled with the liquid collector; 1 and 5) Cones, 2) Main tube, 4) Acrylic support; Letters A-C signal the views drawn below (Figure 12).

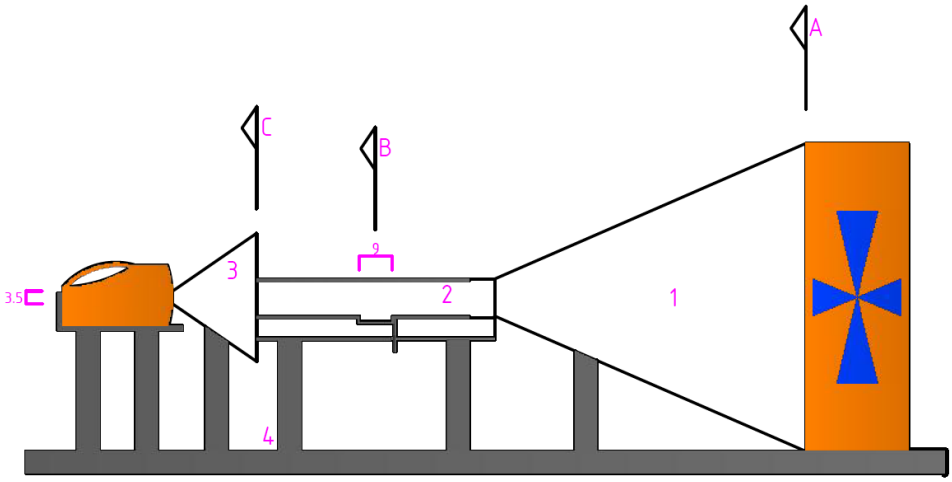

Figure 13 - Side view of the full aerosolization chamber, assembled with the filter collector; 1 and 3) Cones, 2) Main tube, 4) Acrylic support; Letters A-C signal the views drawn below (Figure 14).

The air is captured on the outside, passes through a series of HEPA filters, and only then is available inside the isolated chamber. Since the chamber is large enough for an air flow within that does not change pressure, our working air will simply enter and exit the aerosolizer multiple times. It gets in through the rotor, which has a frequency inverter for speed adjustment. There, it is forced through a piece roughly shaped as a cone (1) (to understand this part, picture a line in the middle of the smaller end of the cone, and at the same time a mark at the bottommost point of the large end of the cone, uniting both markings and removing that bottom off, and attaching a triangular piece to its base), as seen in Figure 14A, from a back perspective.

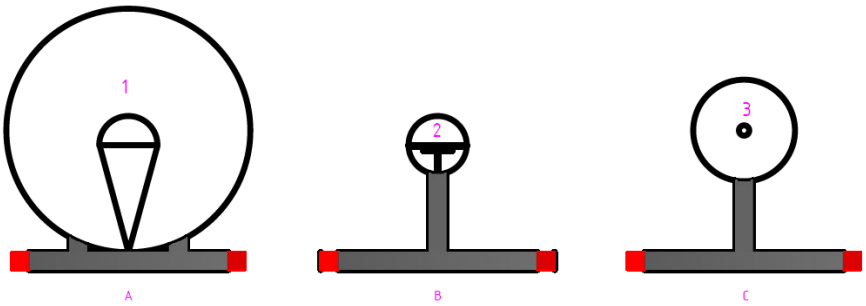

Figure 14 - Back view of the 3 main pieces of acrylic.

After that, it enters our main chamber (2): a hollow tube with a shelf that occupies the whole diameter of the tube. This shelf has a cavity, the size and shape of a petri dish, in order to affix the sample to be aerosolized (Figure 14B). Right before this cavity, there is an orifice with an 8mm diameter, which will allow for the insertion of a digital anemometer. Air flows through the chamber, and out of it, where it will at last find some resistance. Because the machinery that collects the samples has a specific maximum flow, not all the air we are analyzing will pass through to the end. Because of this, the main chamber is not sealed, and instead simply has a cone (3) to channel most of the sample into the direction we are collecting. This way, we do not have to worry about the flow being the same getting inside and out, since it simply escapes after passing the tunnel. This air will be either collected, or recycled into the ventilator again.

An acrylic structure (4) will hold the assembly together throughout the trials, with pillars to sustain each part. Each of the collectors will have a custom shelf, with its own pillars, so the air entrance remains aligned with the exit of the chamber. These pillars should be fixable with simple large bolts like galvanized steel eye bolts, to allow screwing without tools.

Although the chamber already had a sterilization method implemented with peracetic acid, an alternative was found or we would have to use galvanized steel. The solution, that was stable, non-corrosive, and usable both on acrylics and electronic devices, was hydrogen peroxide. The main chamber in acrylic would allow for a full view of the process, and with a simple process, the whole chamber, containing the aerosolizer, could be sterilized.

For logistic and time constrain reasons, none of the chamber was built. Instead, the focus was directed to the detection part, the core biology work that represented the author specialization.

3 Detection system

In the beginning of the design for this simulator, the detection system of choice was a portable magnetoresistive biochip platform, developed at INESC-MN, which uses a surface testing method where the sample is static, and bonded to the surface. This requires surface functionalization tests to be performed, in order to assure the chemical bonds are specific enough using the method and materials chosen.

With the development of the biological methods, and the discussions about the usage of this platform, a shift of interest occurred: an emerging portable platform, using spin-valve cytometry – where the sample is instead flowing and not static, showed itself promising by halving the sample reaction wait times, and with less microfluidic constrains thanks to its permanent bonded chip. For this reason, it was the cytometry platform that was chosen as the detection system, but since some of the surface tests had already been carried out, they were here presented to not only confirm the effectiveness of reagents, but also as a future reference if the project direction shifts again.

Therefore, on this section, only the cytometry system will be detailed. Unless otherwise noted, all microscope images were taken on a Leica DM LM microscope (Leica DFC300 FX camera system).

3.1 Flow cytometry

Flow cytometry is a technique that enables the measurement of morphological, biochemical and functional characteristics of microscopic particles suspended in a stream of fluid. It allows for characterization and quantification at high rates and with a high-throughput[8]. The analysis of the particles can be performed by a different number of ways, from light scattering or staining by fluorophores or quantum dots and having the particles pass through a single-wavelength laser beam or arc lamp[9].

Besides detecting and counting, some cytometers can sort cells at high speeds based on the signal detected, without the sample losing viability or any particle-specific characteristics[10].

The detection platform presented in this work is based on a previously developed system[11,12], as shown in Figure 14. The device is composed of magnetoresistive spin-valve sensors, and functions in conjunction with a microfluidic platform and an amplification & acquisition setup. The sensors have a micrometer spatial resolution and are sensitive to the magnetic field created by magnetized beads flowing in microchannels above them. The detection functions by counting each cell that passes over by giving information on the magnetization of the nanoparticles that flow with them.

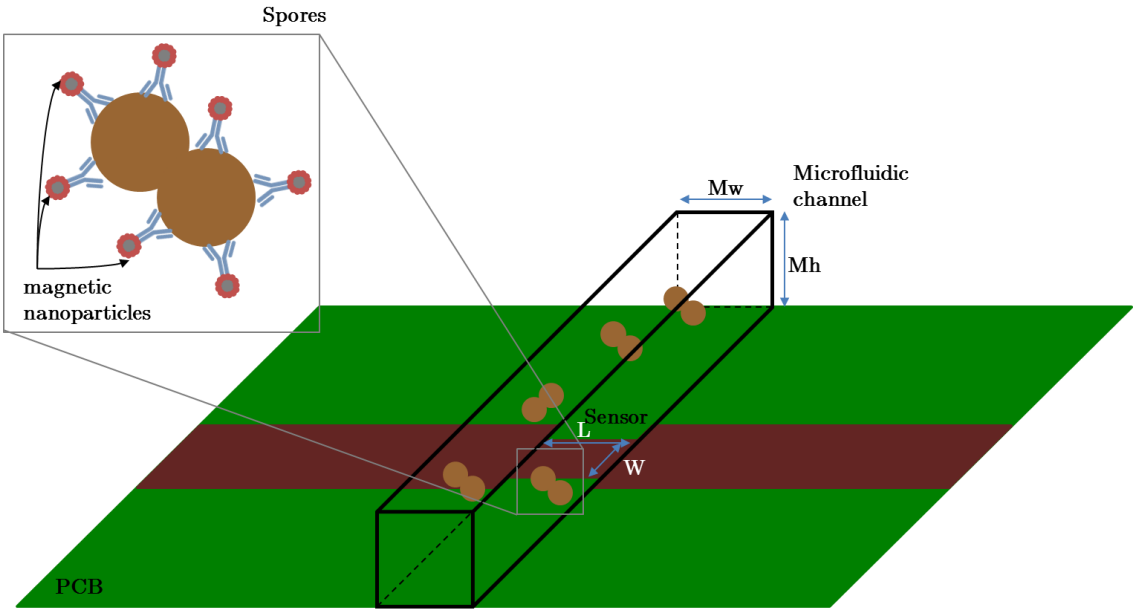

Figure 15 – Schematic of the microfluidic channel that passes over the sensor, where the particles of interest will be detected. L) 100 µm; W) 3 µm; Mw) 100 µm; Mh) 50 µm.

3.2 Magnetoresistive sensors

The spin-valve (SV) sensors used work based on the giant magnetoresistance effect, functioning as linear magnetic field transducers[13]. When patterned by a large aspect ratio, with the long direction at 90 degrees to the pinned layer magnetization easy access, the demagnetizing field changes the alignment of the free layer magnetization, which is at said 90 degrees to the pinned layer easy axis[14]. When affected by a magnetic field, the angle at which the free layer currently is, changes[15](Figure 16).

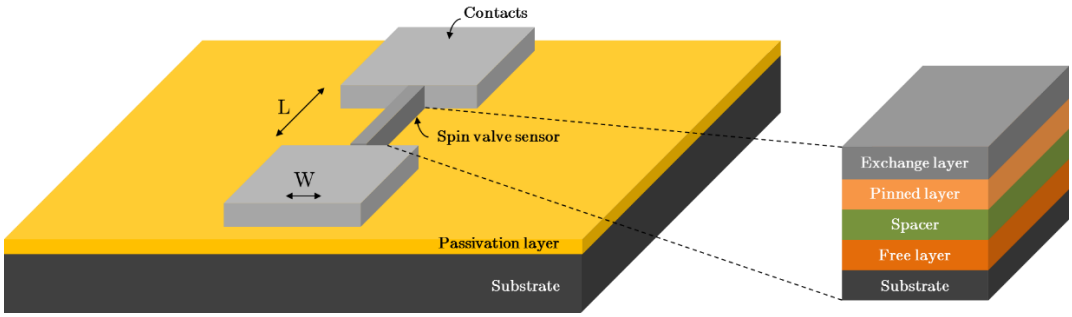

Figure 16 – Schematic of the sensor, and its layers' functionality.

This measured signal is dependent on a number of factors, so a few approximations are made so as to reduce the variables accounted for: the magnetically labeled spores are spherical, the magnetic moment of each spore is the sum of the magnetic moments of the nanoparticles (NP) attached to it, that said NP are evenly spread along the surface of the spores, and that each magnetic particle has a perfect magnetic dipole.

The reaction signal was simulated, and the output voltage calculated using its sensitivity, resistance, dimension, and biasing current, and the MP height, speed, susceptibility and saturation moment, using the following equation,

$$\Delta V = \left(\frac{\Delta R_{max}}{2H_k^{eff}}\right) \times I \times \langle H \rangle_y \quad (1)$$

In (1), ΔR_{max} is the maximum variation of the sensor's resistance (the difference between its resistance when in an antiparallel and parallel state), H^{eff}_k the effective anisotropy field, I is the sensor bias current, and $\langle H \rangle_y$ the y component of the average field over the sensor free layer volume, created by a MP when magnetized by an external field.

Since our particles are not stationary, but instead are moving over the sensor, the magnetic field detected by it will differ with time[15]. In addition, considering a microfluidic rectangular channel, velocities will vary depending on the height at which the spores are passing by, from where different pulses will arise, both in time span and amplitudes (Figure 17).

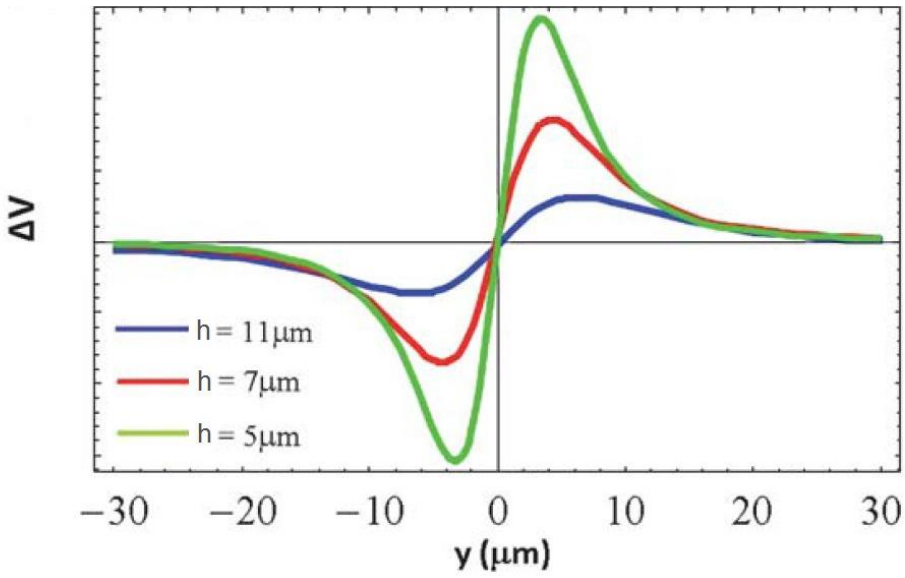

Figure 17 - Signal for cells labelled by uniformly distributed nanoparticles, vertically magnetized, at different heights (5 mm, 7 mm and 11 mm), flowing from left to right.

3.3 Spin-valve layers

The physical platform used in this work was from a previous publication[16], the cytometer platform used was composed of magnetoresistive sensors, readout/acquisition electronics and the microfluidic channel. The device fabrication and layers were based on spin valves (SV) deposited by ion beam deposition on a Nordiko 3000 tool with the following structure:

Si/Al_2O_3 60/Ta1.5/$Ni_{80}Fe_{20}$ 2.5/$Co_{90}Fe_{10}$ 2.0/Cu 2.1/$Co_{90}Fe_{10}$ 2.0/$Mn_{76}Ir_{24}$ 6.0/Ta 5.0 [15,17] (thickness in nm, compositions in atomic %), patterned with 3 μm x 100 μm active dimensions (measured between the AlSiCu 300 nm thick contact leads), as shown in Figure 18. Passivation was done with a 300 nm thick Si_3N_4 layer deposited by PECVD (Electrotech Delta chemical vapor deposition system). Sensors were annealed at 250 ° C for 15 minutes, in vacuum, and cooled under a 1 Tesla magnetic field.

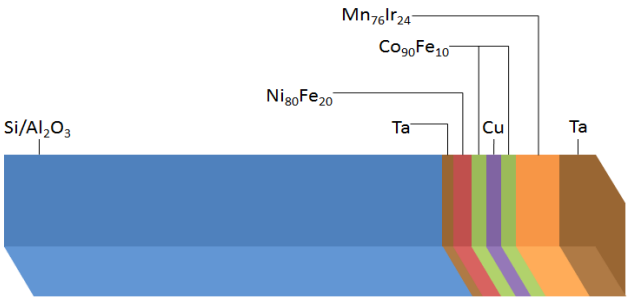

Figure 18 - Spin valve deposition layers, to scale, tilted sideways.

The MP used have a superparamagnetic signature, which means that to activate their magnetization an external vertical field created by a permanent magnet had to be used (NdFeB, 20-10-01STIC, Supermagnete, Gottmadingen, Germany) below the printed circuit board (PCB) (Figure 19). The magnetic field strength at the microfluidic channel center was 31 mT, so the individual nanoparticles were magnetized with a magnetic moment of 2.0 x 10^{18} A.m^2.

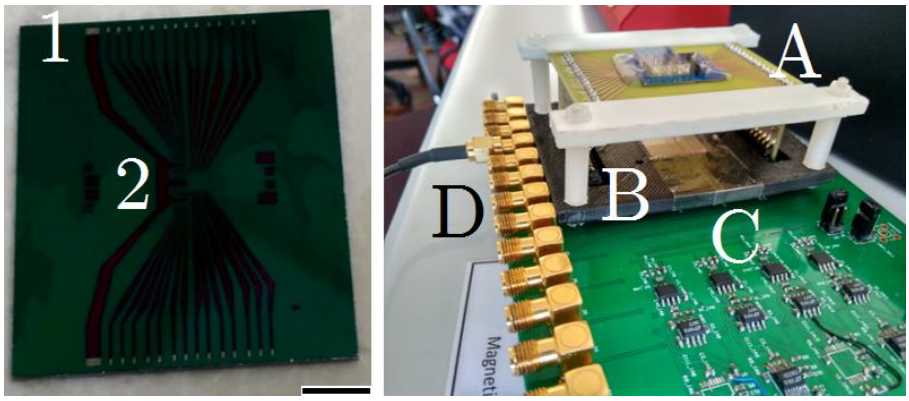

Figure 19 – On the left, the microchip before installation (scale bar = 5mm); 1) Sensor contacts; 2) Spin-valve sensors. On the right, the PCB setup that is shielded in the black box; A) Permanent bonded chip; B) Permanent magnet; C) Amplifiers and filters; D) PCB output channels.

3.4 Chip characterization

The electrical leads were patterned by lithography and liftoff in a 2-contact geometry, and consist of 300 nm thick sputtered Al ($Al_{98.5}Si_1Cu_{0.5}$ in percentages) and 15 nm of TiW(N_2). The sensors have a sensing area of 3 µm x 40 µm (sensor height x distance between electrical leads). They are located at different positions along the length of the channel, positioned between the edges of the full width of the channel (Figure 20).

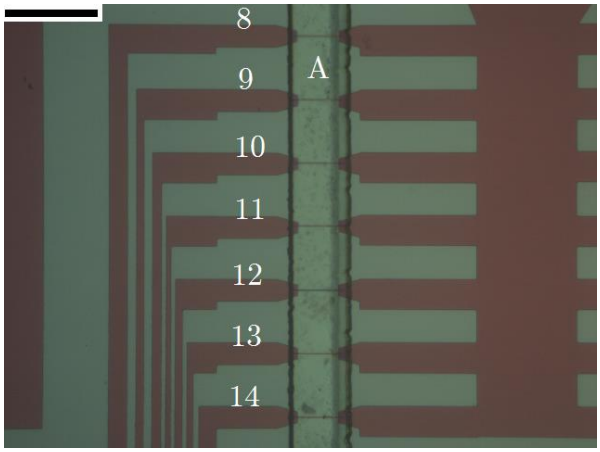

Figure 20 – Sensors and microfluidic channel of the chip (scale bar = 100 μm); 8-14) Sensors; A) Microfluidic PDMS channel.

The characterization response for the 11th SV sensor (transfer curve) is shown in Figure 21, where the magnetoresistive (MR) signal is 8.52% with a sensitivity of 1.32% per mT, leading to a sensitivity of 7.684 $V.T^{-1}$ for a 1 mA bias current.

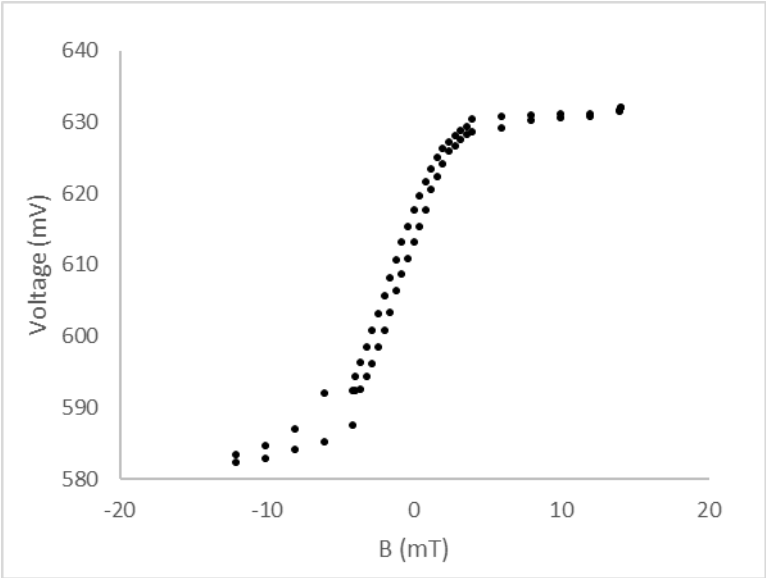

Figure 21 – Transfer curve of a spin valve sensor (MR=8.52%, a sensitivity of 7.684 $V.T^{-1}$ for a 1 mA bias current).

3.5 Magnetic moment for the 100 nm magnetic nanoparticles

The magnetic nanoparticles (84-20-102 micromod BNF-Dextran proteinA coated 100nm) used in the experiments have an iron concentration of 6.0 mg/ml and are coated with dextran. These labels are already functionalized with proteinA. The magnetic moment dependence on field of these particles was measured for a 10 mL sample with a concentration of $6.0x10^{12}$ particles per mL using a Vibrating Sample Magnetometer DMS (Digital Measurement Systems, model 880). This technique is normally used to study the magnetic moment of thin film samples but it can also

be used for solutions containing magnetic particles, the only difference is the holder. A specific quartz reservoir is filled with the solution containing the beads and afterwards is placed on a vertical quartz rod that vibrates along the vertical direction at a frequency *f*.

This movement originates a change of the magnetic flux, inducing a differential of potential in the set of pickup coils placed around the sample. This potential is proportional to the total magnetic moment of the sample. For the magnetic beads sample a total saturation moment of 7.80×10^{-6} A.m^2 was measured for 6.0×10^{10} particles, leading to an individual nanoparticle saturation moment of 1.30×10^{-16}. The nanoparticle magnetization saturates for fields higher than 1 T (Figure 22).

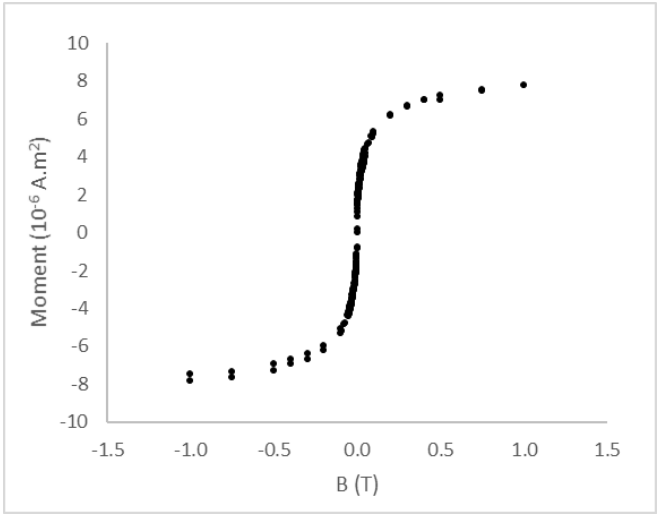

Figure 22 - Magnetic moment of a sample with 6.0×10^{10} MP.

3.6 Microfluidics

The microchannels were fabricated in polydimethylsiloxane (PDMS), with 100 µm (length), 50 µm (height), according to one of the works on the platform[18]. The integration of the magnetoresistive chip with the PDMS microchannels was achieved through irreversible bonding of the Si3N4 and PDMS surfaces. Both surfaces were exposed to ultraviolet/ozone at 28 mW.cm−2 and 5 mm distance from the UV lamp inside the UV-O cleaner machine for 15 minutes and then mounted face-to-face and manually aligned, to be kept at room temperature, overnight. The ensemble was then mounted on the PCB, where the sensors were wire-bonded and the wires protected with silicone (Figure 23).

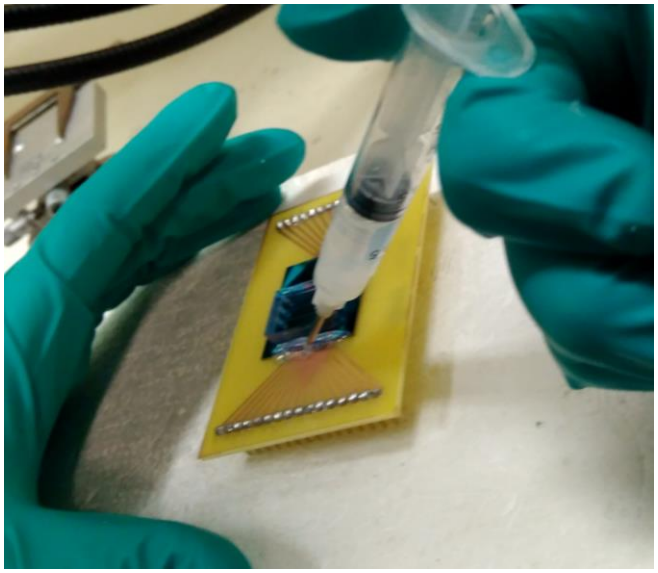

Figure 23 - Protecting of the wire bonding with silicone.

For this particular project, the available biochip was not made from scratch, and not with this application in mind. The microchannel used, although aligned with the sensors, was therefore the only available and viable channel (Figure 23). This would later prove troublesome, as some clogging issues showed up during the measurements.

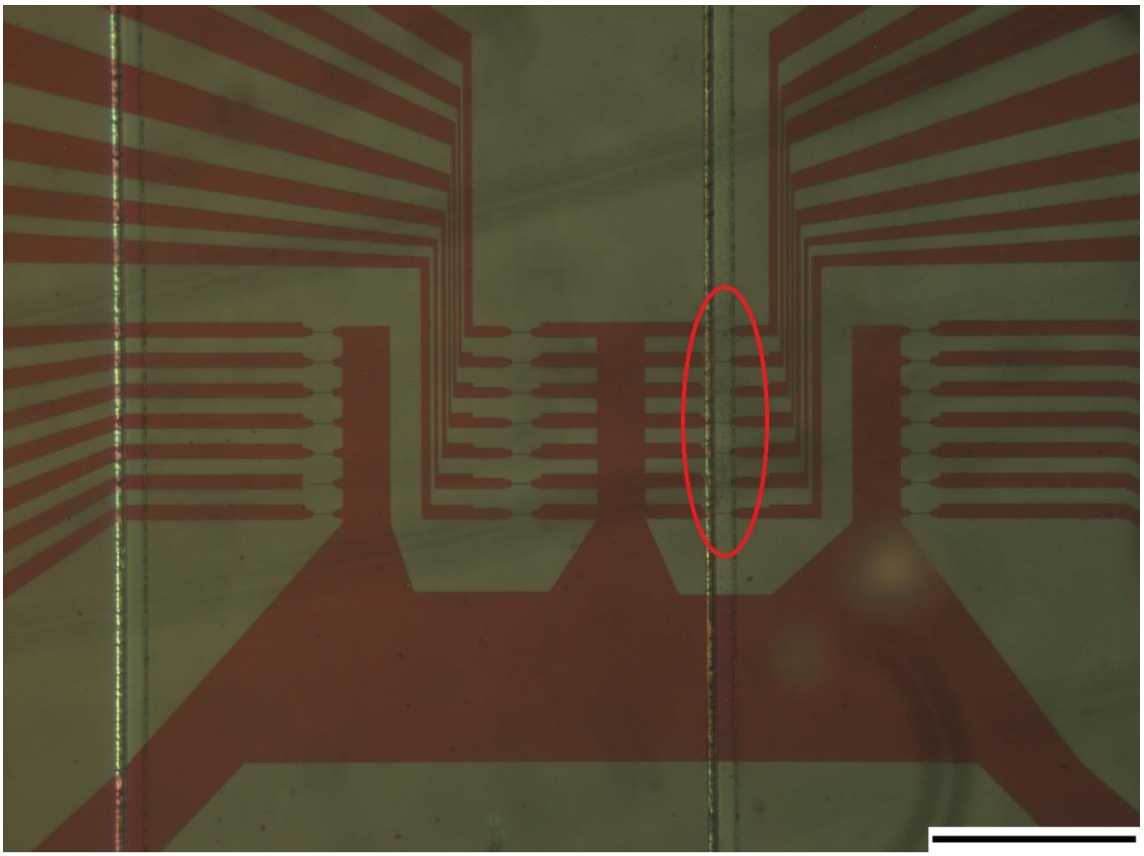

Figure 24 – Microscopic view of the biochip with the PDMS attached to it. As it can be seen by the red ellipse, only one channel is able to be perfectly aligned with the sensors (scale bar = 1mm).

3.7 Electronics

A PCB containing 14 spin-valve sensors was fit on a pin header, and connected to a 5000x gain amplifier with a high-pass filter of 300 Hz and at low-pass filter of 10 Hz, and a configurable DC source ranging from 0.25 mA to 2 mA (Figure 25).

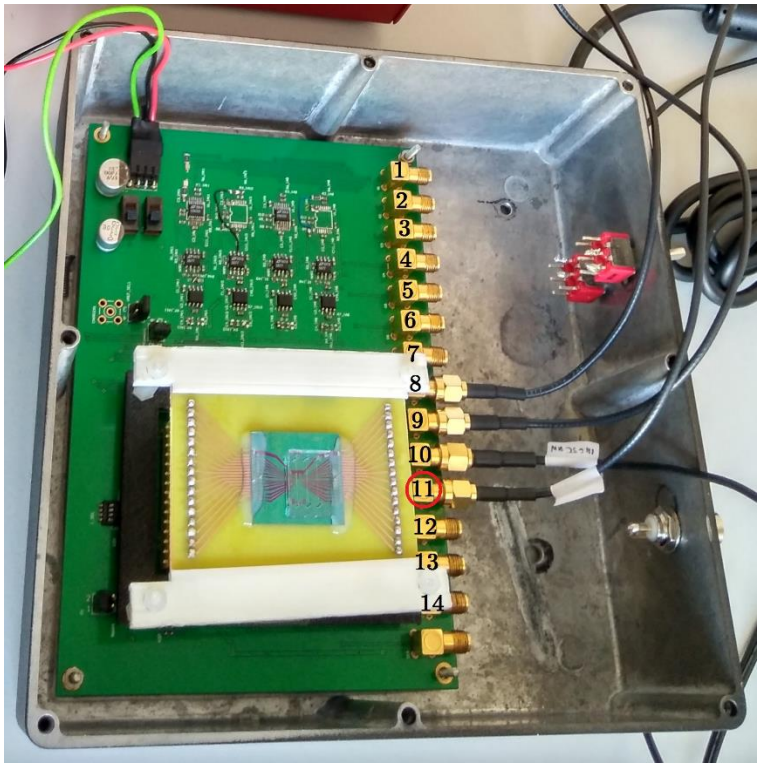

Figure 25 – PCB with the lid open. 1-14) Plugs for the respective sensors; In red, the sensor whose data will be analyzed (plugged to channel 2 of our DAC). Although the 9th sensor is plugged, it was soon discarded as during the trial it gave no readable signal)

The sensor signals were recorded using a 16 bit analog-to-digital converter (ADC board DT9836-12-2-BNC) at a 50 kHz acquisition frequency. Said signals were then processed using a Matlab software, by using a low-pass filter with a cutoff frequency of 2 kHz, storing the acquired data on a laptop (Figure 26). Although the signal noise was minimized by turning off the lights, and the use of DC-current batteries, the noise coming from the ADC power supply was not.

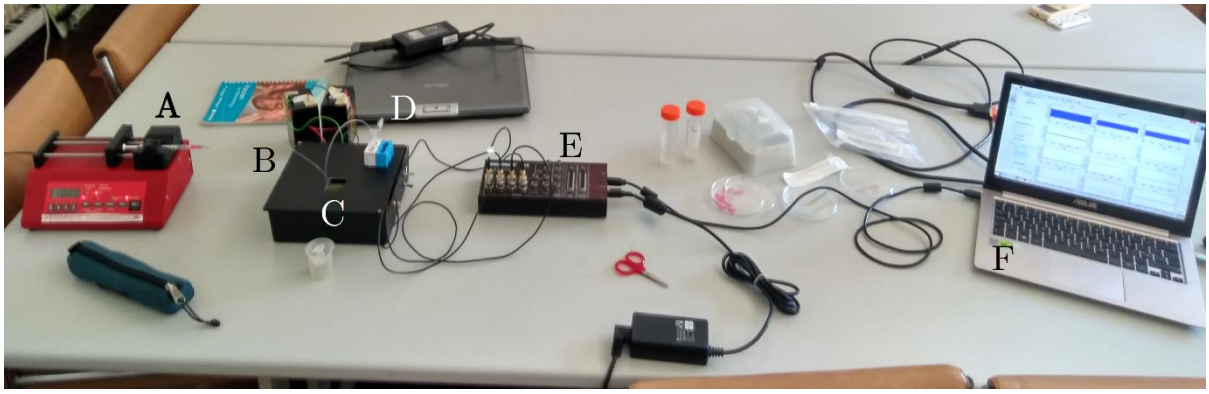

Figure 26 - Full setup for the cytometer. A) Syringe pump and syringe; B) Microfluidic tube inlet; C) PCB box; D) Microfluidic tube outlet (to an Eppendorf); E) Digital-to-Analog converter (plugged by the channels 0, 1 and 2); F) Data acquisition computer (where the 3 top graphics can be seen, representing the channels 0, 1 and 2 – the 8th, 10th and 11th sensor, respectively).

4 Biology

4.1 Summary

Since our detection is based on a series of covalent bonds that connect, ultimately, the target of interest (the spore, in our case) to the magnetic particles, it is essential that we make sure this connection has as much specificity as possible, while ensuring the least amount of sample possible passes by unmarked.

ELISA tests are very accurate thanks to its specificity and sensitivity, especially when compared with other immunoassay tests. To add to these advantages, ELISA requires no radioactive labels or detection equipment, which are in general very expensive. And because a specific antibody highly complementary to our antigen is used, even small amounts of our sample can be marked and detected. It is the reporter group, the enzyme, which needing only a small sample amount (down to the nanogram level) can trigger a number of catalytic reactions that will ensure the full structure assembles.

For this, different surface functionalizations were executed, until a reliable formula was found. All tests were made with negative controls, in order to ensure no false positives were obtained in the end. These surface tests served initially to determine if the formula was usable for the static biochip, but were eventually used only as confirmation that the antibody worked, since it was decided the cytometer would be used.

The reporter group used in this work was not, as normal, biological in nature. By using a magnetic label, nano-sized iron oxide beads, our reporter will not degrade over time, nor will be affected by the sample's chemistry. Turbidity or magnetic background will not be a problem for the magnetic nanoparticles, and none of the expensive fluorescence equipment is needed.

4.2 Surface tests - Sandwich ELISA

A sandwich ELISA was chosen, as there would be no other way of guaranteeing exclusivity in the indirect bonds between the gold surface and the MP, maximizing the amount of antigen connected, eliminating the need to further purify the antigen when real samples are tested, and improving the sensitivity of the assay. For the initial rounds of testing, all biology was confirmed on sandwich surface tests.

Gold was used as a coating agent for its ease of use and connectivity with different proteins, adsorbing to macroscopic gold surfaces via electrostatic and hydrophobic interactions.

Because of this, unintentional bonds might form. Furthermore, since one cannot guarantee the point of connection between antibodies and gold surface, the antibodies might end up in less favorable orientations. To mitigate the undesired orientations, a cross linker was used (Figure 27). Since cross linkers have reactive ends for specific functional groups, one can guarantee only the desired side of a specific substance will adhere to the surface.

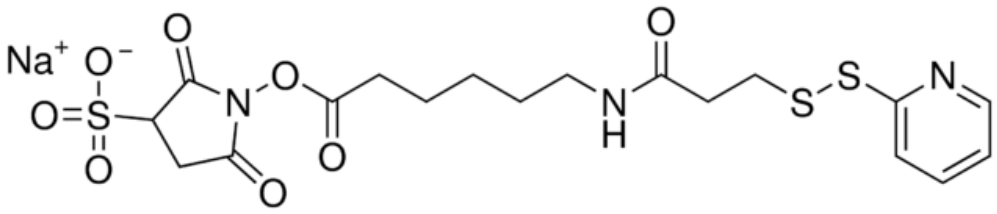

Figure 27 – The linker chosen for the surface functionalization, Sulfo-LC-SPDP (sulfosuccinimidyl 6-[3'-(2-pyridyldithio)propionamido]hexanoate)

Antibodies are organic molecules of folding polypeptide chains, constituted by four protein units, two heavy chains of 50 kDa and two light chains of 25 kDa. These chains are attached by disulfide bridges forming a Y-shape symmetrical structure with amine and carboxyl functional groups as binding sites, as suggested by Figure 28. Each end of the fork contains an identical antigen binding site (keep in mind the antibody is symmetrical, and the different colors simply refer to more characteristics, and as so are shared by both sides).

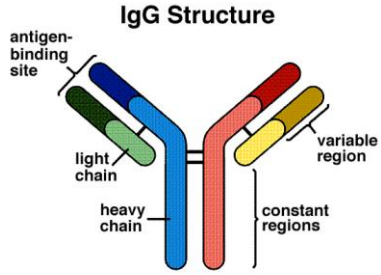

Figure 28 – General structure for an IgG antibody

Our Immunoglobulin G (IgG) antibody is composed of one Fc (fragment crystallizable) structure (the heavy-chain constant region) and two Fab (fragment antigen binding site) fragments (the variable region). This latter region is essential for the formation of immune complexes, as they represent the variable active sites of the molecule that will react with antigens. Antibody-antigen interaction on a solid substrate is also affected by the nature of the spacer between the first immobilized layer and the solid surface.

Protein A will be the connection between our antibody and the magnetic particles. Because our antibody is Protein A purified, it will connect with the magnetic beads used, that are Protein A coated. It is in the Fc region, between the CH_2 and CH_3 domains, that it will bind very strongly with IgG[19].

The last pieces of our complex are the magnetic nanoparticles. As labels, magnetic beads have several advantages. Their magnetic properties are stable over time and they are generally not affected by reagents or light exposure. Moreover, the magnetic background in biological samples is minimal, since they are composed essentially of diamagnetic molecules, and even large magnetic fields are compatible with biochemical processes[20].

As shown in Figure 29, our structure starts off with the gold surface, to which proteins can very easily adhere through hydrophilic and hydrophobic interactions. Since such ease of connection

will result in undesired interactions, a linker is first added, ensuring a predominance followed by a concentrated amount of antibodies, so as to saturate our surface with it. This will consist on the surface treatment, to which the solution containing targets and MP will be added: the target spores will connect, followed by the same antibodies used for the surface treatment, connected to Protein A, which is in turn connected to the MP.

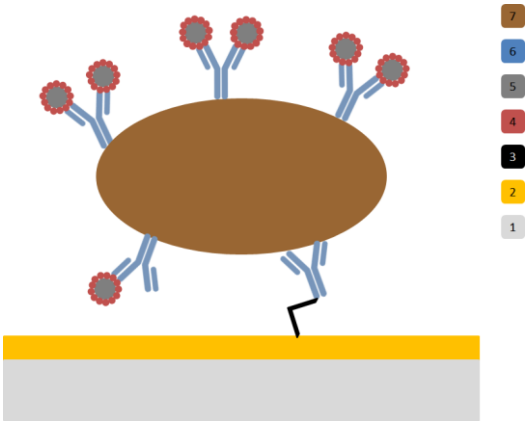

Figure 29 - Representation of the positive sample test performed. 1) Silicon die; 2) Gold cover; 3) Linker; 4) Protein A; 5) Magnetic particles; 6) Antibodies; 7) Spores.

To make sure all false positives are taken into account, 3 other samples will be tested: with no spore, with no antibody (substituted by a BSA surface treatment), and with no spore and antibody (Figure 30).

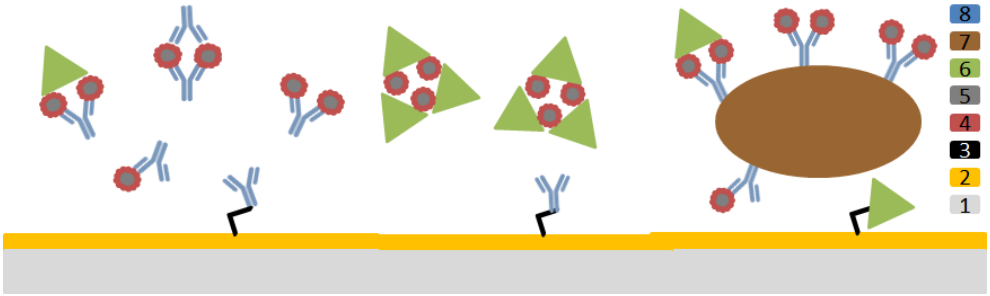

Figure 30 - Representation of the three control tests performed: 1) Silicon die; 2) Gold cover; 3) Linker; 4) Protein A; 5) Magnetic particles; 6) BSA; 7) Spores; 8) Antibodies.

4.3 Suspension trials - Cytometry ELISA

Although the biology of the series of connections between the spores and the magnetic particles will be the same, the real samples that will be analyzed are suspended in a solution, and not bound to a surface. The biology tests conducted in surface were intended to precede the static biochip trials, but after deciding for the cytometer system ended up being a confirmation for all the molecular bonds, by using a brightness and gray scale comparing software (ImageJ, explained in chapter 5.5).

As such, the structures of the two samples that were analyzed are described in Figure 31.

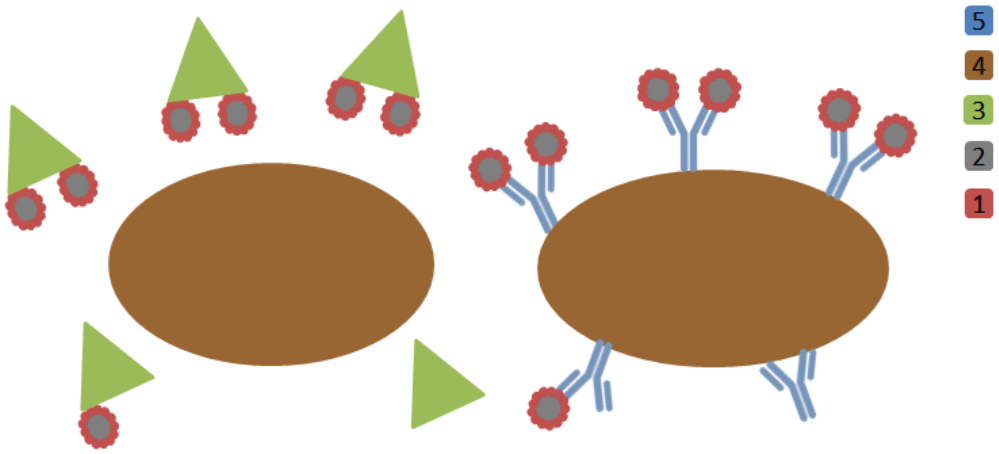

Figure 31 - Representation of the two types of bonding that occur on our two samples: at the left, the Protein A bonds with BSA, therefore not connecting to the spores; to the right, Protein A bonds with the antibodies, and therefore with the spores; 1) Protein A; 2) Magnetic particles; 3) BSA; 4) Spores; 5) Antibodies.

The negative differentiation works because a single MP does not show enough magnetic field to produce a readable signal. As so, only a spore with a lot of MP attached will translate into a filtered signal.

5 Materials and methods

5.1 Solutions used

Unless otherwise noted, all trials were run at INESC-MN Biolab, room 011. Antibodies were acquired from Abcam (ab20556; given its large spectrum of *Bacillus* targets, the immediate availability of the antibodies, and having been referred as functional for the sample spores that were handled) and diluted to 250 µg/ml in a 0.1 M pH 7.4 Phosphate-buffered saline solution (PBS). Spores of *Bacillus thuringiensis* and *Bacillus cereus* were cultivated and purified at LBDB, and diluted to 10^9 CFU/mL, a BSA 5% and BSA 1% solution, both in PBS, was readied, and PBS Tween 0.02% also prepared. Very small gold-coated dies, 7 x 5 mm rectangles (Figure 32) obtained by deposition of a thin (500 Å) film of gold on top of a 16 in silicon wafer that had been previously coated with 50 Å of chromium to promote gold adhesion, and then cut, using a dicing saw, were cleaned with IPA and water (at INESC-MN wet bench in the grey area), using an air gun to dry, and set for 11 minutes in an UVO Cleaner (at INESC-MN grey area). All the surface incubations were carried in simple petri dishes at room temperature. MilliQ water purchased from Millipore® (ultra-pure water), and Isopropyl alcohol (IPA) was bought from Pronalab.

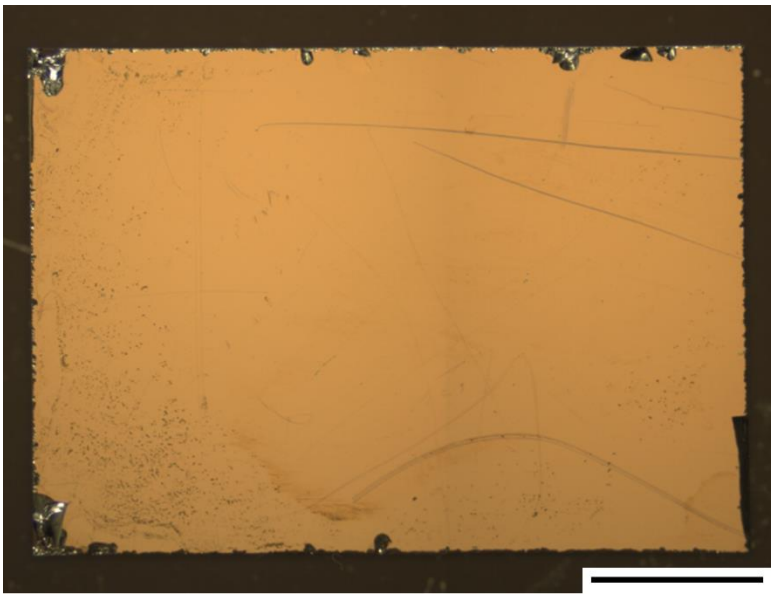

Figure 32 – One of the gold dies used for the surface functionalizations tests (scale bar = 1mm).

5.2 Surface functionalization

A single 2-µl drop of linker was used to spot each of the gold dies (Sulfo-LC-SPDP, bought from Sigma-Arldrich), which were then incubated for 20 minutes. Half the surfaces were then spotted (2 µl) of AB (pDies), and the other half with the same amount of 5% BSA (nDies), followed by a 2 hour incubation. All washing was done twice in PBS Tween and with the help of a magnetic separator.

5.3 Magnetic particles and spores bonding

To be added to the dies after the incubation, two solutions were created in two separate Eppendorf tubes, using 10 µl MP stock solution and 20 µl AB, which were re-suspended, and 100 µl PBS, and set to agitate for 1 hour. They were then washed (Figure 33), and 100 µl 5% BSA was added and incubated for 40 minutes, to ensure the saturation of Protein A bonds. A final wash was executed, and for one of the tubes 20 µl of spores and 80 µl PBS were added (pMix) while for the other 100 µl PBS was added (nMix). Both were set to agitate for 30 minutes, after which they were washed and re-suspended in 20 µl PBS.

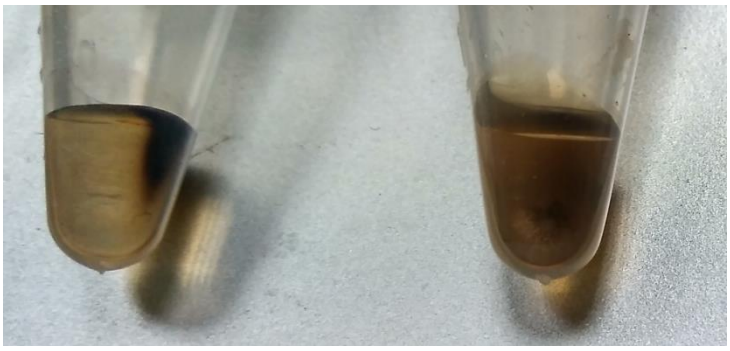

Figure 33 – Separation of the MP in solution, by the magnetic separator. Here, a clear difference can already be seen between the negative, on the left, and the positive sample, on the right.

5.4 Probe - spore binding

Holding by its sides, the dies were soaked in PBS, and left to dry. They were then incubated with 1% BSA for 30 minutes, to further ensure the gold surface would not unintentionally bond, then rinsed with PBS, and 5 µl pMix was added to 3 pDies and 3 nDies, along with 5 µl nMix added to 3 pDies and 3 nDies. They were set to incubate for 30 minutes, and then rinsed with PBS, PBS Tween, and water, let to dry, and analyzed.

5.5 Microscope and ImageJ

The gold dies were analyzed under optical microscopy, using the same values for exposure time (50 ms), gain (1.0x) and color saturation (1.00x), under the 10x objective for the *B. thuringiensis,* and 2.5x objective for the *B. cereus*. Since the black MP are clearly visible once accumulated, it is easy to pick apart the control dies from the positive one. To confirm this differentiation, ImageJ (version 1.51p, USA National Institute of Health) was used as a tool to compare the contrast between the dies. ImageJ is a software that allows for the measure of brightness intensities, or the surface percentage covered by differently colored pixels. To do this, the images were converted to their 8-bit versions, and then thresholded using the same values amongst them, so that the background could be taken off the account. By using the "Measure" plugin, the software was then set to give the area analyzed (Area), the gray scale value – from 0 to 255 (Mean), and the percentage of coverage (%Area).

5.6 Cytometer solutions

After having the biology tested, two solutions were prepared for analysis on the cytometer, based on current INESC-MN work[21,22]. 10 µl MP were placed in an Eppendorf and washed 3 times. After separating, 12 µl PBS was added and put to spin-down for 1 minute. 5 µl of these particles were then added, along with 50 µl PBS to two separate Eppendorf tubes. To one of the Eppendorf tubes (pSample), 10 µl AB were added, while for the other Eppendorf tube (nSample), 10 µl PBS was added. Both were re-suspended, and left to agitate for 1 hour. They were then parted in the magnetic separator, disposed of its liquid content, incubated for 40 minutes with 50 µl 5% BSA. 30 µl of spores were centrifuged for 5 minutes in an Eppendorf tube, and its supernatant disposed. The spores were then washed with 20 µl PBS, re-centrifuged, its supernatant disposed, and 32 µl PBS added; 15 µl of this solution was added to each of the nSample and pSample, after magnetically separating the Samples, along with 85 µl PBS, re-suspended, and put to agitate for 30 minutes. They were then put to spin-down, supernatant removed, and re-suspended in 100 µl PBS. 10 µl was then drained into a tube, for analysis on the cytometer.

5.7 Biosensor analysis

Each trial begins with noise measurement on the sensor by injecting PBS at an initial flow rate of 20µl/min, increased to 50µl/min, and when close to the microchannel reduced again to 20µl/min. Between sampling, the channel was always cleaned with deionized water and then PBS, by increasing flow rate to 90µl/min, and changing the direction of flow if it seemed to clog. The PBS was kept flowing until reaching noise values again, indicating no MP was passing through the sensor. If the flow seemed to halt, its velocity would be gradually increased to 40µl/min, and reduced to the initial value when moving again. Figure 34 shows the software screen, when no fluid was passing through.

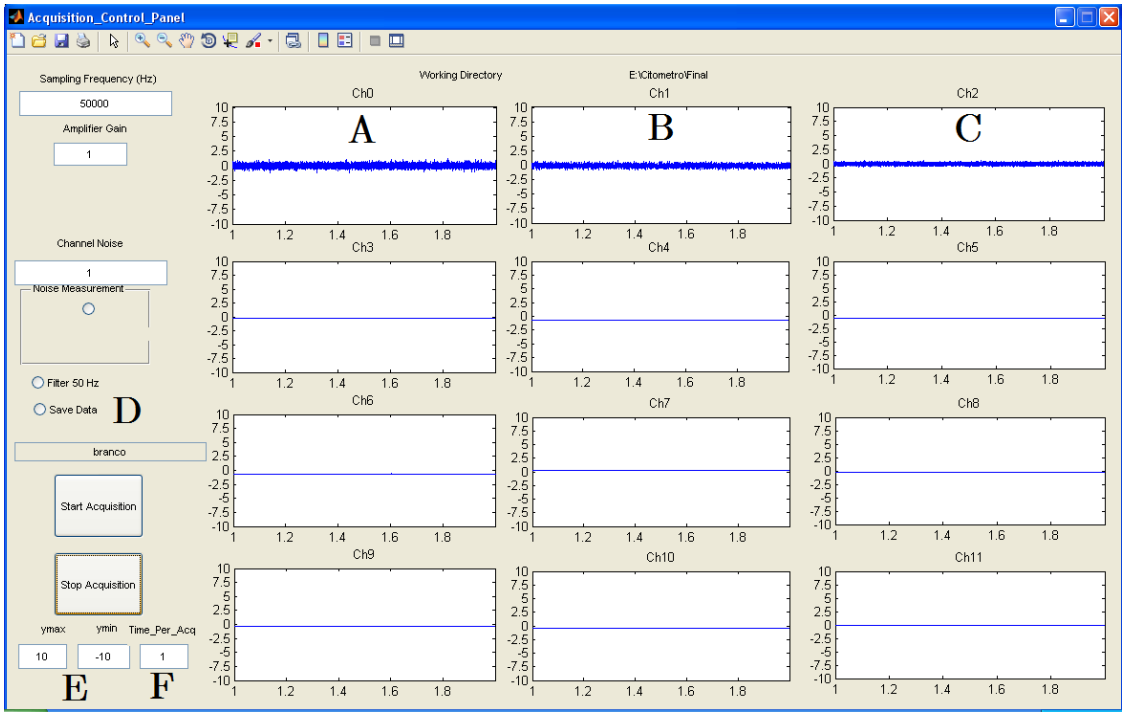

Figure 34 – Cytometer software, stabilized while no fluid is passing. Y axis is the signal in volts×10^{-5}, X axis is time in seconds. A) Channel 0, corresponding to the 8th sensor; B) Channel 1, corresponding to the 10th sensor; C) Channel 2, corresponding to the 11th sensor, the one that produced the data treated later on; D) Saving data option, turned on whenever a sample was being fed; E) Plotting limits for the y axis; F) Time between each data acquisition.

Since the magnetic chip available for use had only 1 microchannel passing through the sensors, all the sampling had to be made on the same one and only inlet. When running, the program was set to measure every 20 microseconds, and would save the acquired signals every 10 seconds.

6 Results

6.1 Antibody, spore and magnetic particle interactions

From the first moment the interactions were tested, it was known that they did indeed work. Because the reagents used were not the same as the ones in both the surface testing and the cytometer, this first experiment on the static platform were not deemed evidence (they followed an existing method from previous INESC-MN work[23]). Yet, standing as the only visual evidence of the microscopic connections, they were chosen to be presented in this work. Figure 35 shows a microscopic image of a biochip used in the static platform, after the first test trial completed, by treating its surface with a 4% formaldehyde solution and letting it sit until dry. The images were captured using a Hitachi Tabletop Microscope TM3030Plus, under 2223 of brightness and a contrast of 1133. Both this first testing trial, and the microscope observation were done at LBDB.

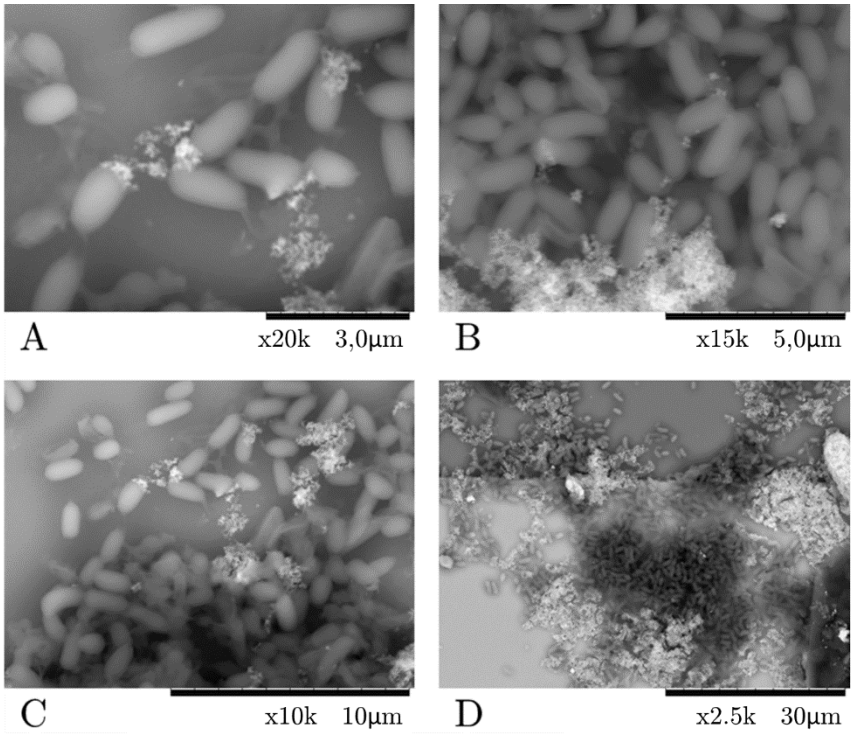

Figure 35 – Chip with sensors, under observation on a scanning electron microscope after the first trial, on 5,000x (A), 10,000x (B), 15,000x (C), 20,000x (D) amplification.

As we can see, there is a clear connection occurring with the spores. Furthermore, there might be a tendency of the antibody to react with the end of the equatorial axis of the spore more easily. Since one of the solutions used at the time was one that promoted some antibody and magnetic aggregation (a PBS Tween solution of much higher concentration), these figures remained inconclusive.

One thing that should be measured, is the maximum number of nanoparticles per cell, which depends primarily on the quantity of both. This can be estimated by measuring the total saturation magnetic moment of a sample magnetically marked, before passing in the SV.

Since for a logistics reason more work was not possible at the time, an estimative of MP saturation was reached by dividing the surface area of a spore by the cross-section area of the MP, rounded up. Following this logic, each spore should have 100 MP available for connection. And so, for each 2.5 µg of spores[24] (1×10^7 CFU), 2.5 µg of antibodies were used, along with 5 µg of MP in each sample.

6.2 First surface testing

In the beginning, it was decided that since the preliminary testing was based on the most recent experiments using the static biochip, the first formula was designed according to it[23] (a method not included in this work, as it was later changed), and only the *B. thuringiensis* spores were tested. Because of this, a high concentration of magnetic particles was obtained on the dies, good enough to produce measurable results, but still having some MP on the negatives. After observation, Figure 36 shows the three negatives and the full sample, along with the ImageJ result obtained.

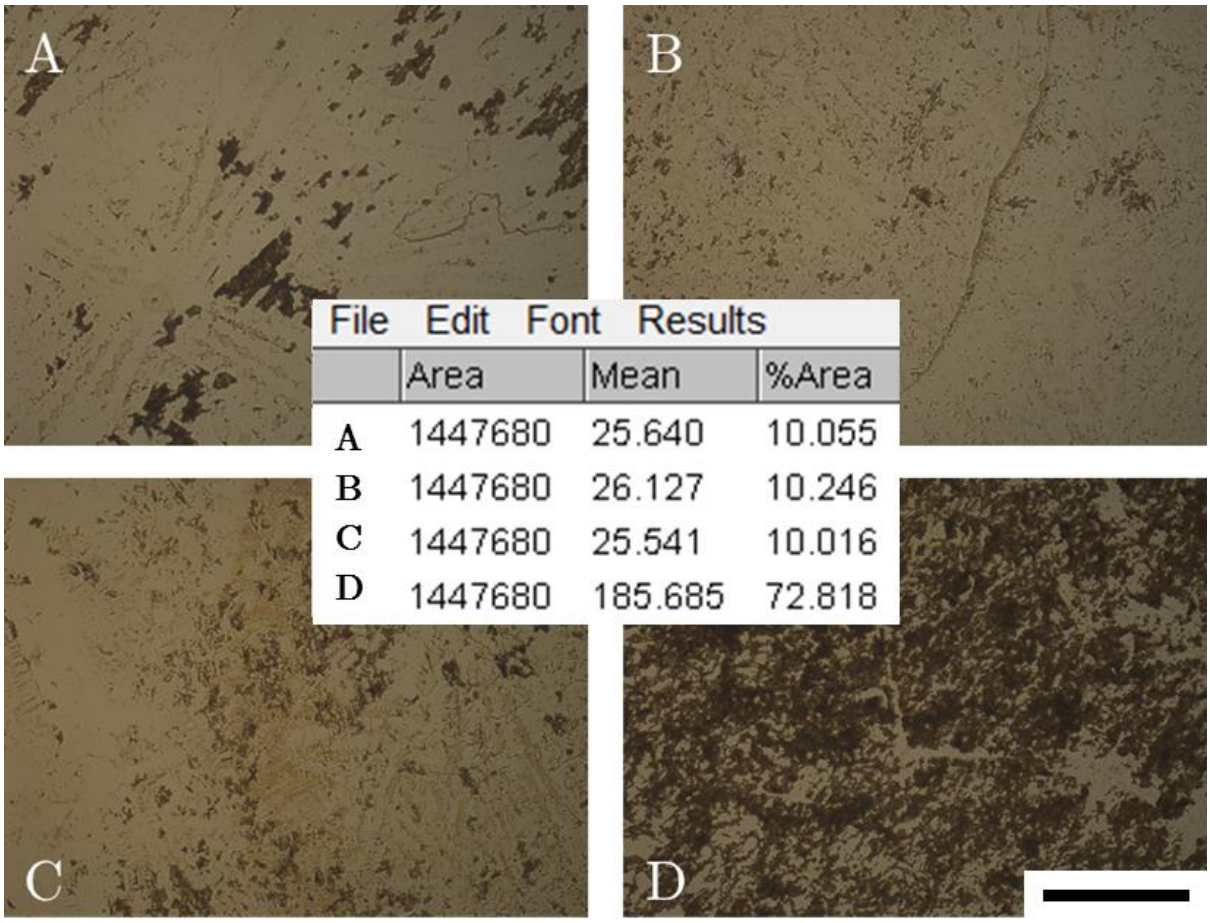

Figure 36 – Surface tests for *B. thuringiensis* (scale bar = 100 µm), and its result from an 8-bit inverted ImageJ grey scale analysis. A) Control without antibody and spore; B) Control without spore; C) Control without antibody; D) Positive test.

As it can be seen even without the numerical analysis, the dies that do not contain both the spores and the antibodies are clearly brighter, and contain far less MP. Upon analysis of the ImageJ

result, we can see the percentage of covered area raises from 10% to more than 72%, thus confirming the biology of the ELISA using that specific antibody, but still showing some signal in the negative dies. It is important to note that the antibody used is sold only as reacting "with spores and vegetative cells of *Bacillus cereus* and *Bacillus subtilis*. Antiserum is unabsorbed and may cross-react with other *Bacillus* species".

6.3 Second surface testing

For the second surface testing, the species *B. Cereus* was used. Here, the final formula was used, chosen to be the one for the static platform tests, if they ever were to be executed, and follow the steps described in chapter 5.1 to 5.4. The results are shown in Figure 37.

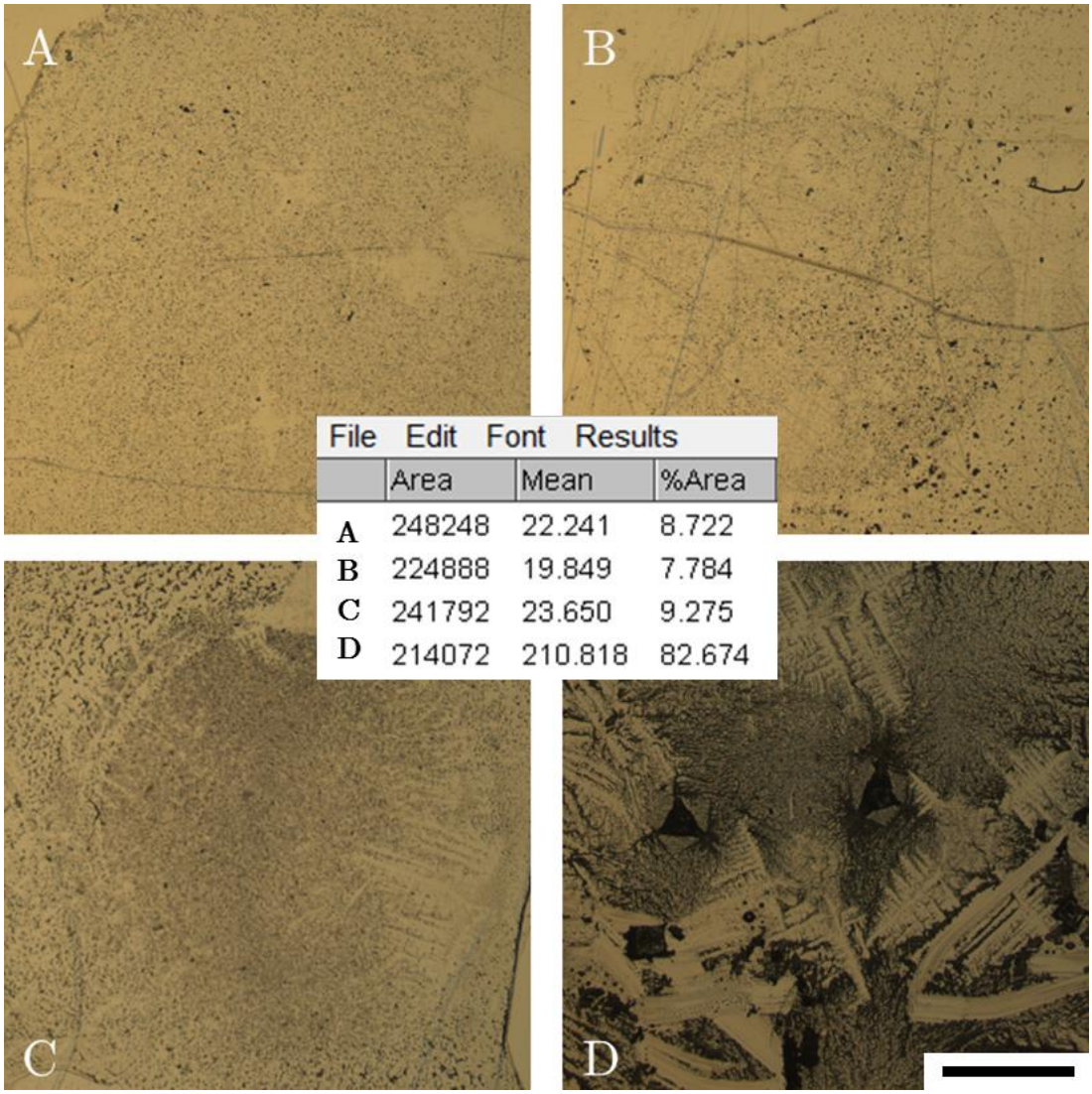

Figure 37 - Surface tests for *B. cereus* (scale bar = 1 mm), and its result from an 8-bit inverted ImageJ grey scale analysis. A) Control without antibody and spore; B) Control without spore; C) Control without antibody; D) Positive test.

Once again, the difference is noticeable at visible eye, and confirmed with the ImageJ analysis of the percentage area covered, that raises from around 9% to over 80%. The antibody was therefore confirmed to be working for our sample of *B. cereus* spores. Although the results were visible, the surfaces still were not blocked 100% efficiently, as our controls still had some surface coverage.

6.4 Running the cytometer

After filling the channel with PBS, the clear sample to later define as noise, the negative sample was passed. Although troublesome at some points, where the flow would halt for some minutes, the negative sample went through completely. The same could not be said for the positive sample. The first thing that was noted, was that the sample was hard to keep homogeneous. Secondly, the flow would halt completely at some points. Finally, after halting for more time than usual, the flow was ordered to increase, in the hopes it would resume normally. Unfortunately, it halted completely, and started to overflow on the microchannel entrance. A quick analysis of the microchip and PDMS revealed the reason, as shown in Figure 38.

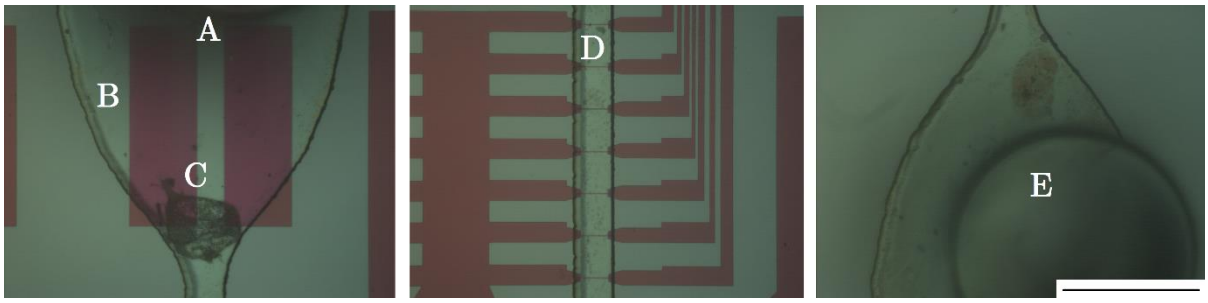

Figure 38 – Chip and microchannel under microscope (scale bar = 50 μm). A) Microchannel entrance; B) Microchannel wall; C) Clogging by an agglomerate of spores; D) Middle of the microchannel, over the sensors; E) Channel exit.

As it can clearly be seen, the channel entrance is blocked by an agglomeration of spores. Whether this was because of poor BSA blocking, the heterogeneity of the solution, or a high spore concentration, we did not know. So the next step, in data treatment, was done with a fraction of the sample, about half of it, since not all of it could pass through the microchannel.

6.5 Running the cytometer – post-analysis

For the data analysis on Matlab, all data files had to first be condensed into one organized file containing the information pertaining to only one sensor, and then, using that file, the average and standard deviation was found and the number and locations of peaks above that pondered average registered, along with the signals plotted. First for the blank sample, secondly for the negative and positive samples. With the blank plot (Figure 39), a noise level was defined as the maximum signal attained while taking into account the standard deviation. With this value (1.978×10-5 volts), the positive sample data (Figure 40) was then plotted while requested to locate all the peaks where the signal was in excess of the noise.

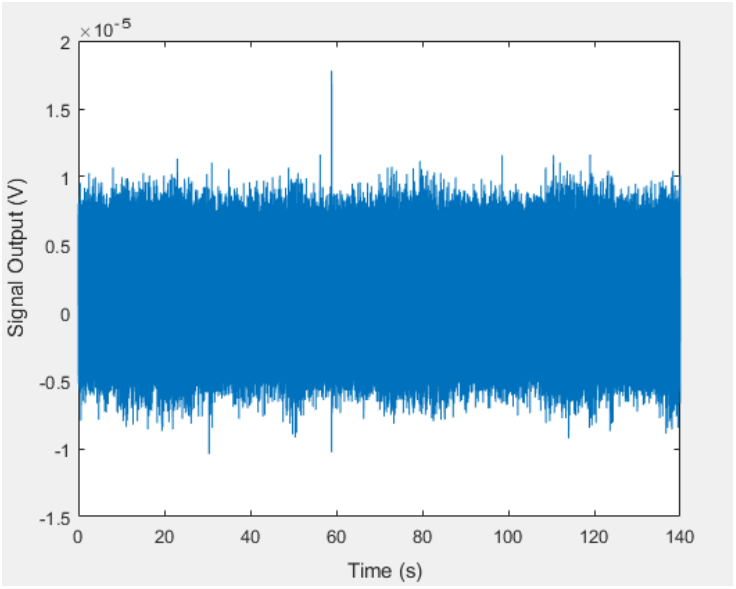

Figure 39 – Plot for the blank PBS sample from the 11th sensor. This was the defining step of our noise level, 1.978×10^{-5} volts, for the peak count afterwards.

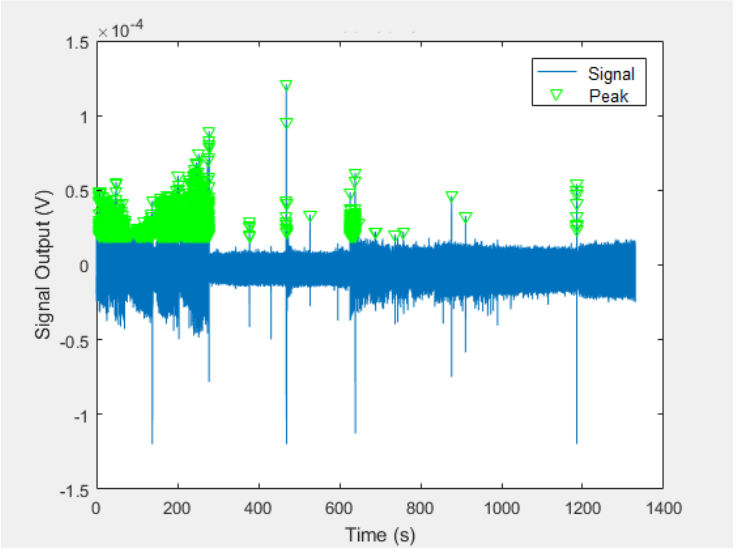

Figure 40 – Plot for the positive (with antibodies) sample from the 11th sensor. In green, we can see the peaks that were located and counted. It can also be seen around where the flow stopped (300s), and where it resumed (650s), unfortunately, not for long enough for all the sample to get through.

As it can clearly be seen, the signal is nowhere near uniformity. At 300 seconds, the peak number drops drastically, as observed before, because the channel clogged, therefore interrupting the flow. For this reason, the analysis was only taken into account while the flow was normal, and the plot and peak count measurement capped at 300 seconds (Figure 40).

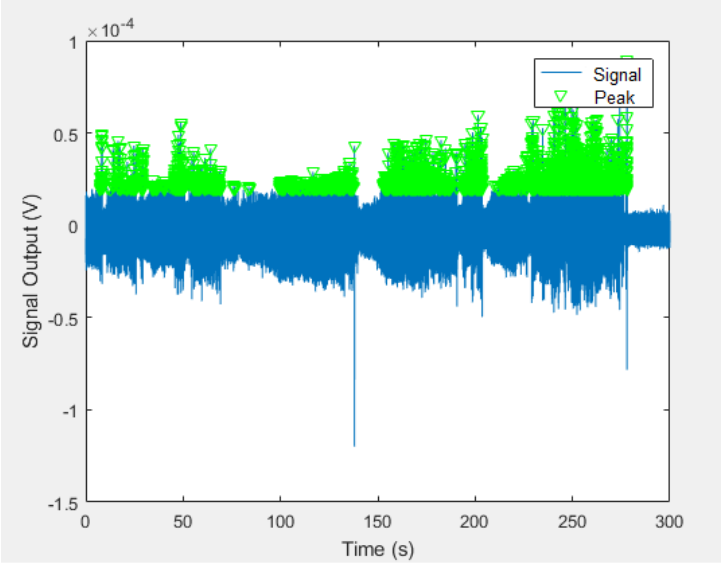

Figure 41 – Plot for the positive (with antibodies) sample for the 11th sensor. In green, we can see the peaks that were located and counted (N=4316).

To make sure there was no misreading of each peak, the scale was further reduced, amplifying the image gradually in order to isolate and observe the curvature of a single peak (Figure 42).

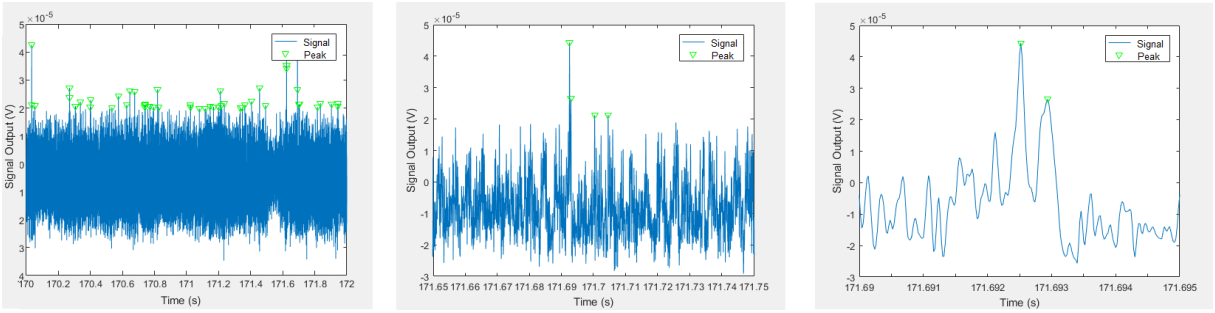

Figure 42 – Plots for the positive (with antibodies) sample for the 11th sensor. In green, we can see the peaks that were located and counted. The scale was gradually reduced in order to zoom in a peak, initially at a 300 seconds interval, to 2, 0.1, and 0.005 seconds (from left to right).

With this, the control sample was plotted under the same conditions, so that a comparable graph and number of counts was obtained. Figure 43 shows the plot for the control sample at the counted limit, and Figure 44 the reduced scale graphs.

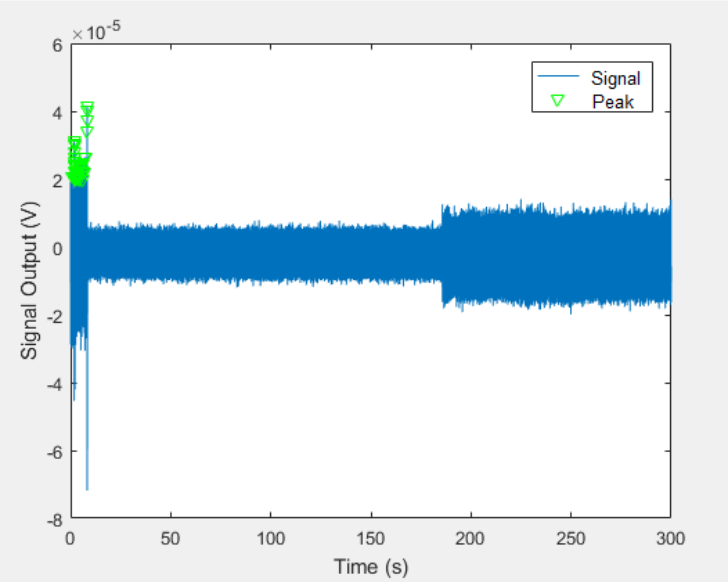

Figure 43 – Plot for the control (no antibodies) sample for the 11th sensor. In green, we can see the peaks that were located and counted (N=53).

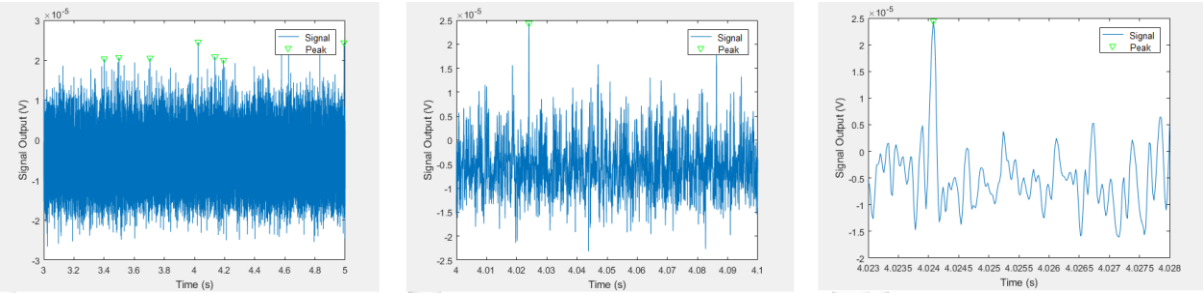

Figure 44 – Plot for the control (no antibodies) sample for the 11th sensor. In green, we can see the peaks that were located and counted. The scale was gradually reduced in order to zoom in a peak, initially at a 300 seconds interval, to 2, 0.1, and 0.005 seconds (from left to right).

As it can be seen from the 300 seconds timeframe, there was just a few starting peaks that managed to be registered. This is most likely due to an agglomeration at the inlet of the microchannel. Unfortunately, the few seconds afterwards are most likely a flow halt, since the signal drops below noise level. Yet, as we observe the flow returning, we do not see peaks, which leaves the question as what provoked the clogging (if it were MP, we would most likely see a peak afterwards).

All the images shown are for data from DAC board channel 2 - 11th SV, and this is because both channels 0 and 1 did not read out good enough signals, for reasons unknown to us (both the SV had good characterization data). To give an example of a bad read, some data from channel 0 – corresponding to the 8th SV, was included in these results (Figure 45). Although some peaks were detected in an even bigger timeframe than the one previously used, they correspond to just over 6% of the total points detected by the 11th SV (depicted above in Figure 41), which used the same number of spores. Considering the method relies on detecting and counting individual spores,

covered in nanoparticles, which pass through the sensor, the 2 channels were excluded from the analysis (the 12th SV offered an even lower count).

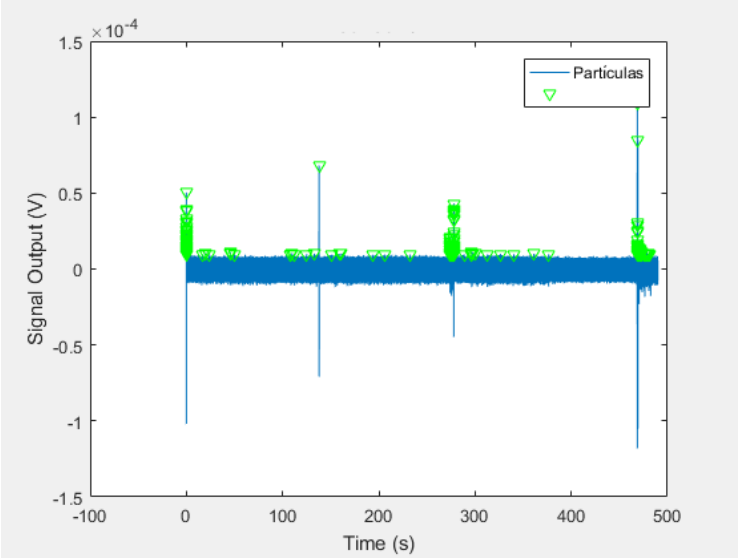

Figure 45 – Failed 8th SV, for the positive sample (N=271).

With a detection difference of 81 times the number of peaks in the control sample (the control yielded 1.23% of the number of peaks in the positive sample), the qualitative tests were completed.

7 Conclusion

This thesis was an ambitious project that started the official collaboration between the two investigating groups, INESC-MN and LBDB. And although the ultimate goal is to achieve a full system capable of simulating and detecting bacterial contaminations, a large amount of brainstorming and logistics work has been performed, particularly in making objectives between the two groups meet, define which goals should be limiting and which we should compromise upon and leave, and what guidelines and layout to look for in future development. It should be noted that although de design dimensions was not defined, most of the work and time spent revolved around the design of the system, always changing each time an obstacle came in the way. The dimensions mentioned in it are basically the only limitation, and other than shape and size caps, they were not defined as to leave flexibility for its decision. Finally, a detection method has already been found, defined, and tested to validity.

In the third chapter, two different detection systems were compared and although the cytometer was the electronic readout of choice for this work, it should not be a limiting option for the development of this project. Since the first step was to confirm the method would indeed detect the sample, the quickest way would be the cytometer, and since the final goal would be of a continuous system, it was the obvious choice.

At the fourth chapter, two different surface tests were presented, one for each *Bacillus* species. Because these were preliminary tests, the concentrations were set a bit higher than what probably would be the best conditions. Also, some controls had some adherence. As stated in the respective section, this is most likely due to an inefficient BSA blocking, but should be explored further. The linker usage should also be confirmed, and if not, eliminated altogether.

On chapter 5, the cytometer platform was used. Different concentrations should now be tested here, and a calibration curve for the amount of spores vs signal should be created. A starting detecting range was now proven to work, and the concentrations should now be reduced to find out if there are no clogging issues, or if it really is a blocking or agglomeration problem. A reliable software and hardware system should also be developed and acquired, to minimize any memory errors, and time analysing data.

Spores of *Bacillus thuringiensis* and *Bacillus cereus* at 6.43 μg/ml and 7.58 μg/ml (10^7 CFU/ml) were chemically bound with success to gold dies as surface tests, using a formula developed in this work. On the cytometry platform, *Bacillus thuringiensis* at the same concentration was analyzed using a method based on these surface tests, and successfully detected, yielding a spore count of 4,316 for around 300,000 spores the sample contained (when taking into account that less than 10% of the sample got through the microchannel). Although still a low number for an individual counting platform, the results differentiate with significance from the control count (53), setting therefore a threading path for a correlation between peak number and number of spores. Dilutions of 1000, 100 and 10 times the final solution would be recommended, as to try and find at which concentration interval does the negative yield a less proportional count, followed by raising and lowering the concentration from -5x to 5x in small steps to give the best spore detection range.

Future approaches to this project should include assembling and ordering the simulation system, testing and calibration of its spore aerosolization rate vs concentration, and extensive testing on the detection system, so that the best method for quantification is found and the optimization work is centered on the simulations.

Nonetheless, this work stands off as a proof of concept for a spore detection system using the spin-valve flow cytometry platform, and as a preliminary design for a malign contamination simulation chamber.

8 References

1. Anthrax Attributes -Biological Weapons. Available at: http://www.globalsecurity.org/wmd/intro/bio˙anthrax-att.htm. (Accessed: 10th July 2017)
2. Chauhan, S. S. *Biological weapons*. (APH, 2004).
3. Hoeber, A. M. & Douglass, J. D. The Neglected Threat of Chemical Warfare. *Int. Secur.* **3,** 55 (1978).
4. Reshetin, V. P. & Regens, J. L. Estimating Bacillus Anthracis Spore Dispersion in a High-Rise Building. *J. Eng. Phys. Thermophys.* 1–10 (2004).
5. Mullett, C. A. & Raj, P. K. A User's Manual for ADAM (Air Force Dispersion Assessment Model). Volume 2. (1990).
6. SASS 2300 Wetted-Wall Air Sampler for Indoor and Outdoor Monitoring. Available at: http://www.resrchintl.com/SASS˙2300˙air˙sampler.html. (Accessed: 31st May 2017)
7. Sartorius MD8 Airport Portable Air Sampler MD8; Airport; Portable:Diagnostic. Available at: https://www.fishersci.com/shop/products/sartorius-md8-airport-portable-air-sampler-md8-airport-portable/14555867#. (Accessed: 1st June 2017)
8. Simonnet, C. & Groisman, A. High-Throughput and High-Resolution Flow Cytometry in Molded Microfluidic Devices. *Anal. Chem.* **78,** 5653–5663 (2006).
9. Yu, H.-W., Kim, I. S., Niessner, R. & Knopp, D. Multiplex competitive microbead-based flow cytometric immunoassay using quantum dot fluorescent labels. *Anal. Chim. Acta* **750,** 191–198 (2012).
10. Piyasena, M. E. & Graves, S. W. The intersection of flow cytometry with microfluidics and microfabrication. *Lab Chip* **14,** 1044–59 (2014).
11. Loureiro, J. *et al.* Magnetoresistive chip cytometer. *J. Appl. Phys.* **109,** 2255–2261 (2011).
12. Freitas, P. P. *et al.* Spintronic platforms for biomedical applications. *Lab Chip* **12,** 546–557 (2012).
13. Freitas, P. P., Ferreira, R. & Cardoso, S. Spintronic Sensors. *Proc. IEEE* **104,** 1894–1918 (2016).
14. Oliveira, N. J. R. G. de. Spin-valve heads for tape applications. (unpublished doctoral dissertation, Instituto Superior Técnico, 2000).
15. Freitas, P. P., Ferreira, R., Cardoso, S. & Cardoso, F. Magnetoresistive sensors. *J. Phys. Condens. Matter* **19,** 165221 (2007).
16. Duarte, C. *et al.* Semi-Quantitative Method for Streptococci Magnetic Detection in Raw Milk. *Biosensors* **6,** 19 (2016).
17. Gehanno, V. *et al.* Ion beam deposition of Mn-Ir spin valves. *IEEE Trans. Magn.* **35,** 4361–4367 (1999).
18. Fernandes, A. *et al.* Lab-on-Chip Cytometry Based on Magnetoresistive Sensors for Bacteria

Detection in Milk. *Sensors* **14,** 15496–15524 (2014).

19. Silva, A. *et al.* Linearization strategies for high sensitivity magnetoresistive sensors. *Eur. Phys. J. Appl. Phys.* **72,** 20 (2015).

20. Llandro, J., Palfreyman, J. J., Ionescu, A. & Barnes, C. H. W. Magnetic biosensor technologies for medical applications: a review. *Med. Biol. Eng. Comput.* **48,** 977–998 (2010).

21. Fernandes, E., Dias, T., Cardoso, S. & Freitas, P. P. One-step trapping of droplets and surface functionalization of sensors using gold-patterned structures for multiplexing in biochips (unpublished manuscript, 2017).

22. Cherre, S. *et al.* Rapid and specific detection of cell-derived microvesicles using a magnetoresistive biochip. *Anal.* **44,** 1–7 (2003).

23. Valentim, J. P. P. Optimization of a Lab-On-Chip Device to Study the Biocementation of Soils. (unpublished master's thesis, Instituto Superior Técnico, 2016).

24. Carrera, M., Zandomeni, R. O. & Sagripanti, J.-L. Wet and dry density of *Bacillus anthracis* and other *Bacillus* species. *J. Appl. Microbiol.* **105,** 68–77 (2008).

9 Annexes

9.1 Biochip fabrication

Run Sheet for Magnetic Counter fabrication process

RUN:

Process Start : **Process Finish :**

SV#_____ = MR=___ % Hf= ___ Oe

STEP 1	**1st Exposure –** Spin valve Definition	Date:

Substrate: Si substrate with 1000 Å of SiO2 and passivated SV

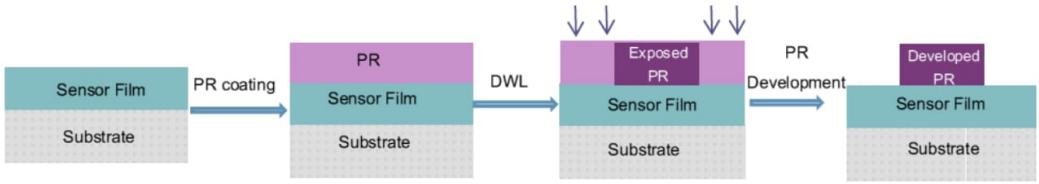

1) Coating PR: Vapor Prime 30 min (Recipe - 0) - Organic compound (Hexamethyldisilane, C6H18Si2)
This step promotes the PR coating adhesion.

Step description	Conditions
Wafer dehydration	Vacuum, 10 Torr, 2 min. N2 inlet, 760 Torr, 3 min. Heating to 130°C
Priming	Vacuum, 1 Torr, 3 min. HMDS, 6 Torr, 5 min.
Purge prime exhaust	Vacuum, 4 Torr, 1 min. N2 inlet, 500 Torr, 2 min. Vacuum, 4 Torr, 2 min.
Return to atmosphere	N2 inlet, 3 min.

2) Coat 1.5 µm PR (Recipe 6/2) - Positive photoresist (PFR7790G27cP - JSR Electronics)

Coating Parameters	
First Step	Dispense photoresist on the sample and spinning at 800 rpm for 5 sec.
Second step	Spin at 2500 rpm for 30 s to obtain ~1.45µm thickness.
Third step	Soft bake at 85°C for 60 seconds.

3) Machine: DWL 2.0

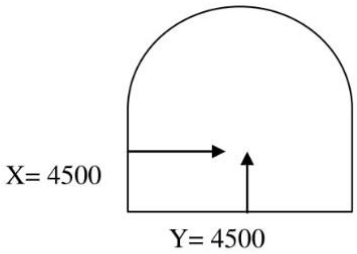

Mask: inesc_citometro_2.0.dwg Map:

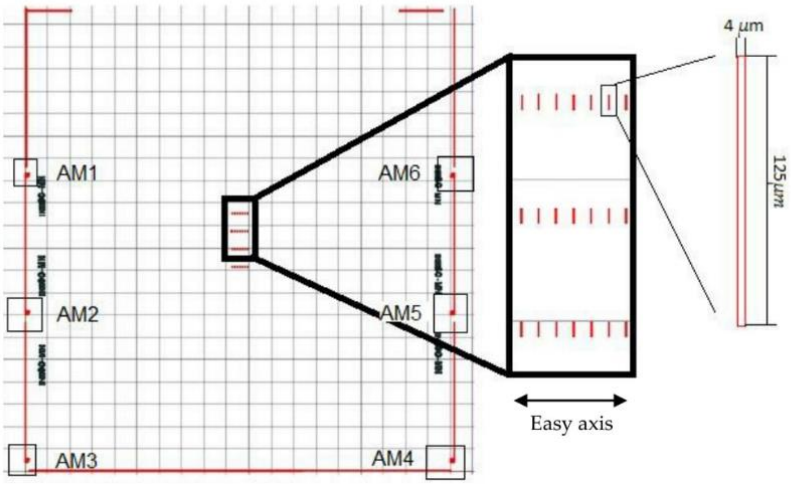

Alignment mark position:

AM1	X= 162.06 Y= 16483.42
AM2	X= 169.06 Y= 8833.48
AM3	X= 162.06 Y= 570.42
AM4	X= 23938.06 Y= 570.42
AM5	X= 23950.06 Y= 8833.48
AM6	X= 23946.06 Y= 16483.42

Energy: 55

Power: 100 mW

Focus: -20

Alignment mark points

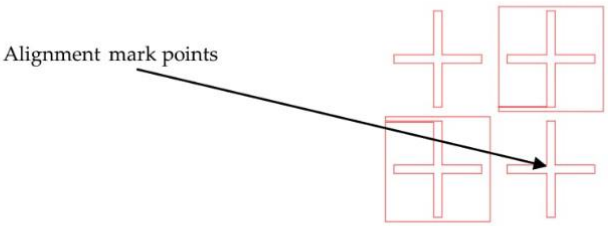

4) Develop : Recipe 6/2

Developer: TMA238WA

Development parameters:
Bake at 110°C for 60s
Cool for 30s
Developer for 60s

5) Inspection:

STEP	Comments
1	
2	
3	
4	

STEP 2	**Ion Milling –** Spin valve etching	Date:

Machine: Nordiko 3600 Ion beam deposition and milling system

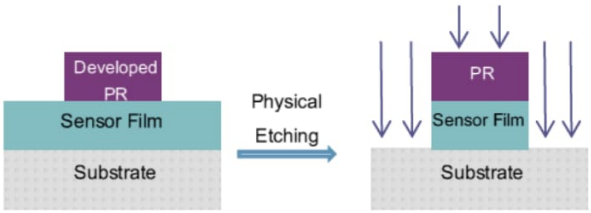

Total thickness to etch: 345 Å
Etch rate: ~ 1 Å/s **Required time:** 400 s

Standard Etching Recipe (junction_etch) : Junction_etch

Assist Gun	Power (W)	V+ (V)	I+ (mA)	V- (V)	I- (mA)	Ar Flux (sccm)	Pan (deg)	Rotation (rpm)
Set Values	150	735	105	-350	-	10	60	30
Read Values								

Inspection:

Comments

STEP 3	**Resist strip**	Date:

Equipment: Wet bench

1) **Microstrip® at 65ºC + ultrasounds**

Started:
Stoped:
Total Time in hot µ-strip :
Ultrasonic Time :

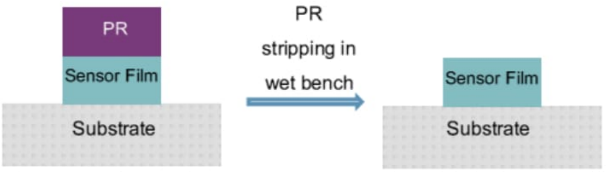

2) **Rinse with IPA + DI water + dry**

Inspection:

Comments

STEP 4	**2nd Exposure –** Contact	Date:

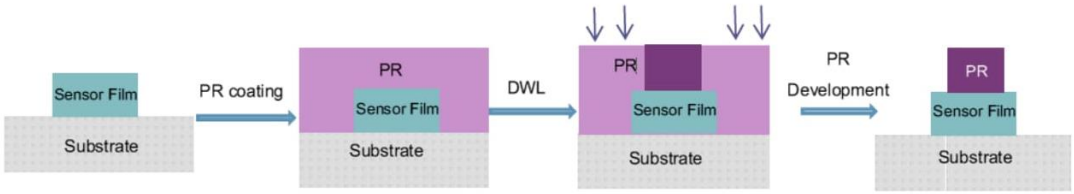

1) Coating PR: Vapor Prime 30 min (Recipe - 0)

Step description	Conditions
Wafer dehydration	Vacuum, 10 Torr, 2 min. N2 inlet, 760 Torr, 3 min. Heating to 130℃
Priming	Vacuum, 1 Torr, 3 min. HMDS, 6 Torr, 5 min.
Purge prime exhaust	Vacuum, 4 Torr, 1 min. N2 inlet, 500 Torr, 2 min. Vacuum, 4 Torr, 2 min.
Return to atmosphere	N2 inlet, 3 min.

2) Coat 1.5 μm PR (Recipe 6/2)

Coating Parameters	
First Step	Dispense photoresist on the sample and spinning at 800 rpm for 5 sec.
Second step	Spin at 2500 rpm for 30 sec. to obtain ~1.45μm thickness.
Third step	Soft bake at 85ºC for 60 seconds.

3) Pre-development Developer: TMA238WA

Pre-development parameters:
No bake
Developer for 20s

4) Machine: DWL 2.0

Mask: inesc_citometro_2.0.dwg Map:

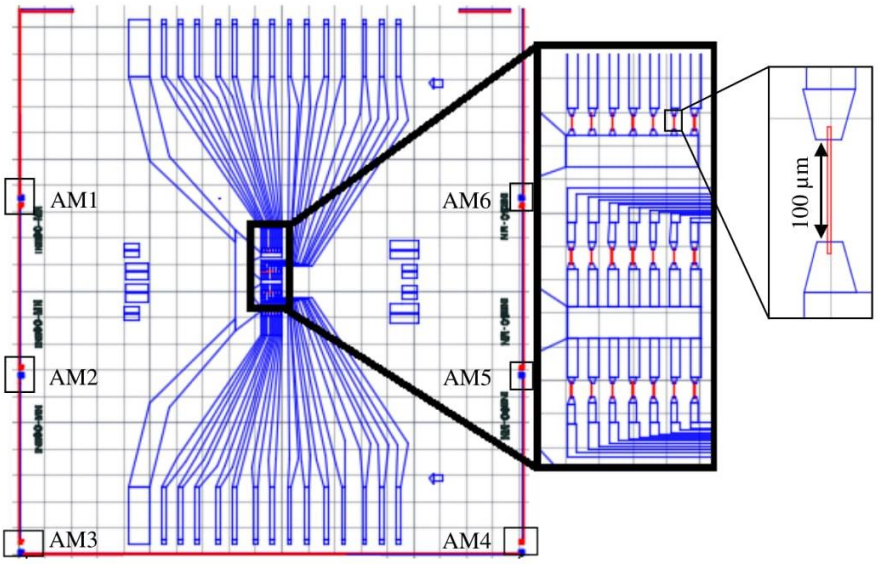

Alignment mark position:

AM1	X= 162.06 Y= 16483.420
AM2	X= 169.06 Y= 8833.48
AM3	X= 162.06 Y= 570.42
AM4	X= 23938.06 Y= 570.42
AM5	X= 23950.06 Y= 8833.48
AM6	X= 23946.06 Y= 16483.42

Energy: 55 + 20 %

Power: 100 mW

Focus: -20

Alignment mark points

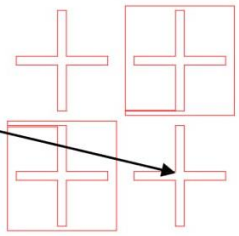

5) Develop : Recipe 6/2 Developer: TMA238WA

Development parameters:
Bake at 110°C for 60s
Cool for 30s
Developer for 60s

6) Inspection:

STEP	Comments
1	
2	
3	
4	
5	

STEP 5	**Contacts deposition**	Date:

Machine: Nordiko 7000
Expected thickness: 3000 Å (Al) + 150 Å (TiWN2)

Module 2– f.9 (1′ soft sputter etch)					
	Power1 (W)	Power2 (W)	Gas flux (sccm) Ar	Pressure (mTorr)	
Set Values	60	40	50	3	
Read Values					

Module 4 – f.1 (3000 Å Al, 1′20′′)					
	Power (kW)	Voltage	Current	Gas flux (sccm) Ar	Pressure (mTorr)
Set Values	2			50	3
Read Values					

	Module 3 – f.19 (150 Å TiWN2, 27′′)					
	Power (kW)	Voltage	Current	Gas flux (sccm) Ar	Gas flux (sccm) N_2	Pressure (mTorr)
Set Values	0.5			50	10	3
Read Values						

Inspection:

Comments

STEP 6	**Aluminum Lift-Off**	Date:

Equipment: Wet bench

1) **Microstrip® at 65ºC + ultrasounds**

Started:
Stoped:
Total Time in hot µ-strip :
Ultrasonic Time :

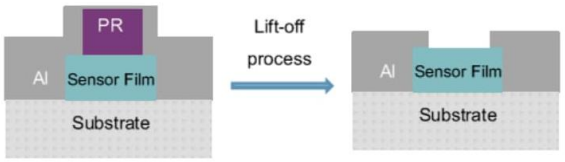

2) **Rinse with IPA + DI water + dry**

3) **Inspection:**

Comments

STEP 7	**Passivation layer - 3000Å Si_3N_4**	Date:

Machine: Electrotech Delta Chemical Vapor Deposition System
Expected thickness: 3000 Å
Time: 1min 14 sec
Holder: 300ºC
Showerhead: 350ºC

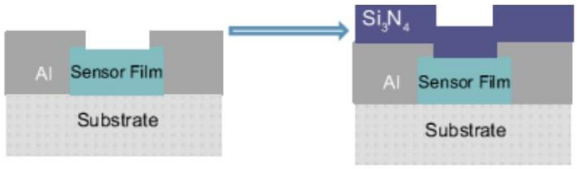

	Deposition Time	**SiN thickness (A)**	**NH_3 gas flux (sccm)**	**SiH_4 gas flux (sccm)**	**N_2 gas flux (sccm)**	**Pressure (mT)**	**Power Source RF (W)**
Set Values	1min 14 sec	3000	500	300	3500	850	500
Read Values							

Inspection:

Comments

STEP 8	**3rd Exposure –** passivation layer	Date:

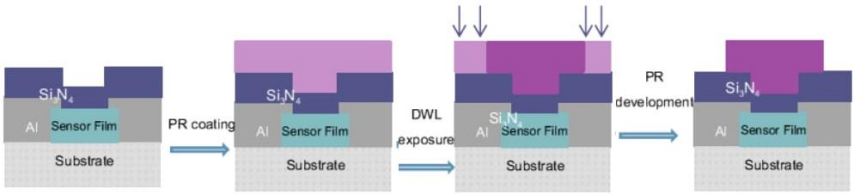

1) Coating PR: Vapor Prime 30 min (Recipe - 0)

Step description	Conditions
Wafer dehydration	Vacuum, 10 Torr, 2 min. N2 inlet, 760 Torr, 3 min. Heating to 130°C
Priming	Vacuum, 1 Torr, 3 min. HMDS, 6 Torr, 5 min.
Purge prime exhaust	Vacuum, 4 Torr, 1 min. N2 inlet, 500 Torr, 2 min. Vacuum, 4 Torr, 2 min.
Return to atmosphere	N2 inlet, 3 min.

2) Coat 1.5 µm PR (Recipe 6/2)

Coating Parameters	
First Step	Dispense photoresist on the sample and spinning at 800 rpm for 5 sec.
Second step	Spin at 2500 rpm for 30 sec. to obtain ~1.45µm thickness.
Third step	Soft bake at 85ºC for 60 seconds.

3) Machine: DWL 2.0

Mask: inesc_citometro_2.0.dwg Map:

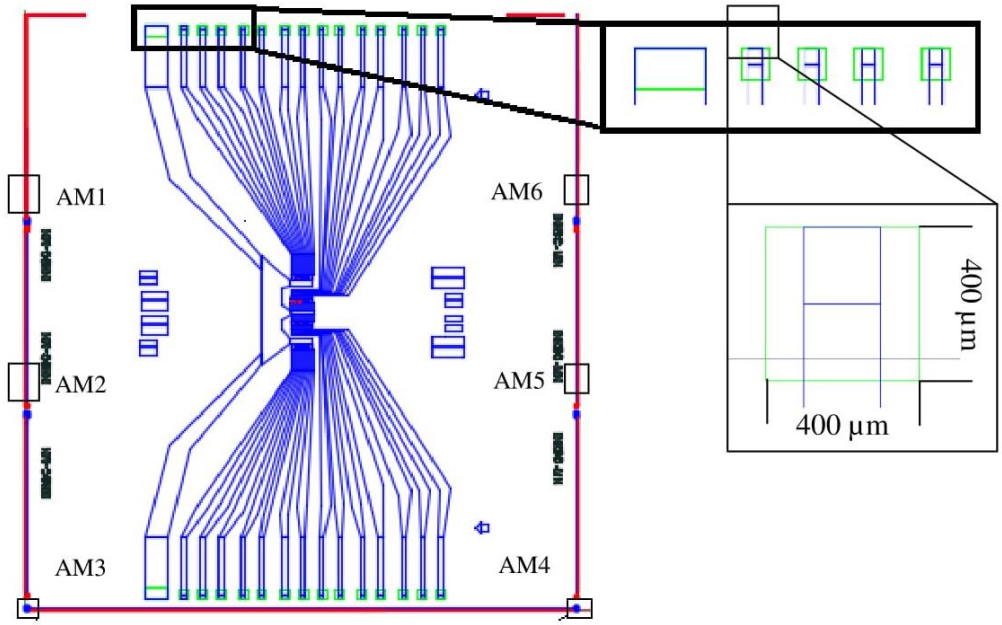

Alignment mark position:

AM1	X= 162	
	Y= 16831	
AM2	X= 165	
	Y= 8443	
AM3	X= 162	
	Y= 54	
AM4	X= 23946	
	Y= 54	
AM5	X= 23946	
	Y= 8443	
AM6	X= 23946	
	Y= 16831	

Alignment mark points

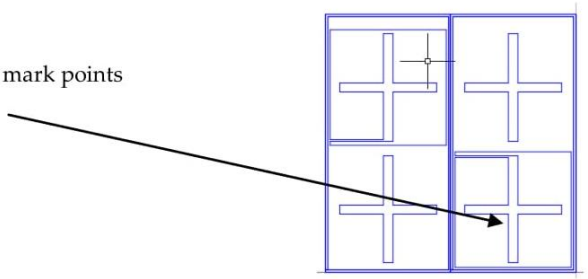

Energy: 55 Power: 100 mW Focus: -20

4) Develop : Recipe 6/2 Developer: TMA238WA

Development parameters:
Bake at 110°C for 60s
Cool for 30s
Developer for 60s

Inspection:

Comments
Confirm that photoresist is everywhere except over the vias

STEP 9	**Reactive ion etching –** pads openning	Date:

Equipment: LAM Rainbow 4400
Process recipe: 6
Expected thickness: 3000 Å
Thickness to etch: 3000 Å
Etch rate: ~ Å/s
Second step: Time – 5 x 230s

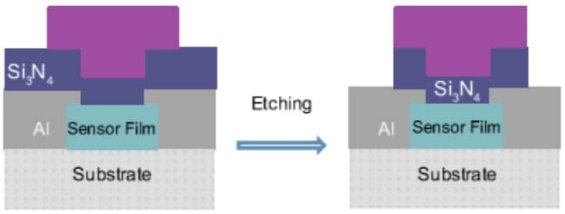

Etching conditions:

	Pressure (Torr)	Etch time (s)	Power (RF)	Ar Flux (sccm)	CF_4 Flux (sccm)	O_2 (sccm)
Expected	140 mTorr	-300 s *-over-etch*: 300s	100 W	200	100	0
Observed		- -cooling: *-over-etch*:	s s s			

Inspection:

Comments
Measure resitance before resist cleaning

Next step: annealing
A) if sample needs annealing -> maintain resist –> dice –> clean –>
B) if sample needs no annealing -> resist strip –> dice –> clean

STEP 10	**Dicing**	Date:

Machine: **DISCO DAD 321**

Die size: X = 23994 + 0 (separation) ; Y = 25856 + 0 (separation)

STEP 11	**Resist strip**	Date:

Equipment: Wet bench

1) Microstrip® at 65ºC + ultrasounds

Started:
Stoped:
Total Time in hot µ-strip :
Ultrasonic Time :

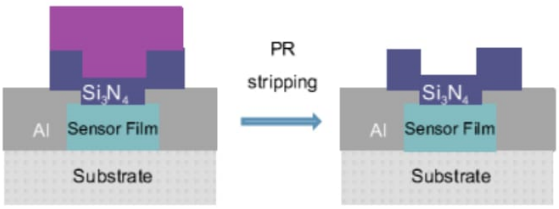

2) Rinse with IPA + DI water + dry

3) Inspection:

Comments

STEP 12	**Annealing**	Date:

Equipment: 21100 Tube Furnace (BL Barnstead Thermolyne) and a 1T magnet.

Annealing conditions:

1) Heating the sample till 250°C then leave it 15min@ 250 °C.

2) Annealing for 1h @ 250°C, under a magnetic field of 1 kOe.

9.2 PDMS handling

PDMS mixture and curing.

Step 1: PDMS mixture

Date:	Operator:	Pre-treatment: No

Substrate: Silicon substrate from 6 in wafers <100> with PR

Equipment: Scale, plastic cup and plastic spoon, dessicator

Mixture conditions:

Step 1.1:Mix PDMS: curant in 10:1 weight ratio and mix well.

Step 1.2: Degass for 1h (using the exicator) or until bubbles disappear.

Observations:

Step 2: PDMS casting

Date:	Operator:	Pre-treatment: No

Substrate: Silicon substrate from 6 in wafers <100> with PR

Equipment: Oven

Mixture conditions: Procedure occurs inside a laminar flow chamber (avoid contaminations)

Step 2.1: Place the SU-8 mold in the respective PMMA holders.

Step 2.2: Hold the PMMA plates together using strong office springs. The plates are pressed against the SU-8 mold to avoid PDMS leaks.

Step 2.3: Inject the PDMS through the PMMA holes using a Luer Lock syringe and a blunt needle.

Step 2.4: Cure the misture inside an oven for 1h at 60 °C.

Step 2.5: Wait for some time before removing the PDMS from the mold.

Observations: Check the channels with the microscope.

PDMS bonding: Microchannel bonding to glass/sensor surface.

Step 1: Cleaning

Date:	Operator:	Pre-treatment: No

Substrate: Counter chips and PDMS

Step 1.1: PDMS cleaning

Rinse with IPA and deionized water and dry with nitrogen

Step 1.2: Chips cleaning

Submerge the chips in Microstrip2001 at 60 °C for 2h if they have photoresist on it.

Rinse thoroughly with deionized IPA and water and dry with nitrogen

Observations:

Step 2: Oxygen Plasma

Date:	Operator:	Pre-treatment: No

Substrate: Counter chips and PDMS

Equipment: UVO CLeaner (Model 144AX-220, Jelight Company, Inc.)

Conditions: 15min

	Machine	Plasma Conditions	Time
Expected	UVO cleaner	28mW/cm^2, 5mm separation from UV light (ozone plasma)	10min+5min exhastion step
Observed			

Observations: Immerse the PDMS bonded with Chip in water after the process.

Step 3: Alignment

Date:	Operator:	Pre-treatment: No

Substrate: Counter chips and PDMS

Equipment: Alignment platform (inside clean room)

Conditions:

Fix the chip to the micropositioner and then place the PDMS on top of it (always dispensing ethanol between both surfaces).If necessary add more ethanol during the alignment.

Place the surfaces in ethanol enabling them to slip relatively to each other and to maintain the activation as long as possible. During the alignment, the PDMS mold is fixed with an incorporated pair of tweezers while the chip is fixed to the translation stage allowing it to have a translational movement until the alignment crosses from both pieces match.

Leave it to dry at room temperature overnight, in clean room.

Step 3: Wire bonding

Date:	Operator:	Pre-treatment: No

Substrate: Counter chips and PDMS

Step 11.1: Drill holes in the PCB (using a 0,8mm tool). Then weld metallic pins to the PCB.

Step 11.2: Glue the die on a PCB using H3 glue.

Step 11.3: Mounting of one die (magnetoresistive chip and microfluidic platform) on a PCB by wire bonding (uses ultrasonic vibrations to weld aluminum wires to the contacts on the chip).

Step 11.4: Wire bonding is covered with silicone gel (applying a soft gel cover over the wires and then allowing it to harden by drying for 3-4h at room temperature).

Observations:

9.3 Antibody datasheet

abcam

Product datasheet

Anti-Bacillus cereus antibody ab20556

★★★★★ 2 Abreviews

Overview

Product name	Anti-Bacillus cereus antibody
Description	Rabbit polyclonal to Bacillus cereus
Specificity	Reacts with spores and vegetative cells of Bacillus cereus and Bacillus subtilis. Antiserum is unabsorbed and may cross-react with other Bacillus species.
Tested applications	**Suitable for:** ICC/IF
Species reactivity	Bacillus cereus Bacillus subtilis
Immunogen	Purified spores of Bacillus cereus (ATCC 11778) and Bacillus subtilis (ATCC 9372).

Properties

Form	Liquid
Storage instructions	Shipped at 4°C. Upon delivery aliquot and store at -20°C. Avoid freeze / thaw cycles.
Storage buffer	Preservative: 0.1% Sodium Azide Constituents: 0.01M PBS, pH 7.2
Purity	Protein A purified
Clonality	Polyclonal
Isotype	IgG

Applications

Our Abpromise guarantee covers the use of **ab20556** in the following tested applications.

The application notes include recommended starting dilutions; optimal dilutions/concentrations should be determined by the end user.

Application	Abreviews	Notes
ICC/IF	★★★★★	Use at an assay dependent dilution.

Target

Relevance	Bacillus cereus is a Gram-positive, facultatively aerobic sporeformer whose cells are large rods and whose spores do not swell the sporangium. These and other characteristics, including biochemical features, are used to differentiate and confirm the presence B. cereus, although

	these characteristics are shared with B. cereus var. mycoides, B. thuringiensis and B. anthracis. Differentiation of these organisms depends upon determination of motility (most B. cereus are motile), presence of toxin crystals (B. thuringiensis), hemolytic activity (B. cereus and others are beta hemolytic whereas B. anthracis is usually nonhemolytic), and rhizoid growth which is characteristic of B. cereus var. mycoides.
Cellular localization	Bacterial spore

9.4 Surface tests protocol

Run Sheet for Biology Surface Testing

Operator: Trial:

Date:

Location:

- Laminated chamber (if toxic/pathogenic), PDMS room, basement room #020
- Biolab, basement room #011

Material / Reagents / Equipment:

- Magnetic separator
- Automatic mixer
- Microscope and ImageJ
- Linker
- Magnetic Particles solution (MP; concentration:) in PBS
- Sample (concentration:)
- Sample' s antibodies (AB; concentration:) in PBS
- BSA 1% solution in PBS
- BSA 5% solution in PBS
- PBS solution
- PBS Tween 20 0.02% solution
- Paper towel for cleaning
- Two plastic cups
- Three Eppendorf tubes
- Three gold-coated pieces per condition (total 12)
- Isopropyl alcohol (IPA) for cleaning
- Distilled water for cleaning
- Gloves

Process Time: 4h30

Process:	**Time:**
Location: Table or laminated chamber	**Operator:**

1) **Surface:** Clean the gold die with IPA and water. Use air gun to dry.
2) Place 11 minutes in the UVO Cleaner.
3) Ready all solutions at the desired concentrations.
4) Place a single drop of linker (2 µL) on the gold surface and incubate for 20 minutes at RT in a humidity chamber.
5) Spot (2.5 µl) the surface with both the AB and 5% BSA. Immobilize for 2h in a humidity chamber.
6) **Mix:** Place 10 µL of the MP (don' t forget the stock particles have to be washed) to two new Eppendorf tubes.
7) Add 20 µL of the antibodies solution.
8) Re-suspend and mix the solution.
9) Add 100 µL of PBS Tween.
10) Mix and agitate for 1 hour.
11) Wash and add 100 µl of 5% BSA. Incubate for 40 min.
12) Wash and add 20 µl of the spore solution, followed by 80 µl of PBS for the positive samples. For the negative ones, wash and simply add 100 µl of PBS. Agitate for 30 min.
13) **Surface:** holding by the handling end of the Biochip, or the sides of the gold-coated pieces, soak it in PBS. Clean around the contacts (in the PCB area).
14) Wait until it dries, and the bubbles disappear.
15) Incubate with 1% BSA in PBS for 30 min.
16) **Mix:** Wash in PBS Tween, and re-suspend in 20 µl PBS.
17) **Surface**: Rinse with PBS. Add 20 µl of the prepared **Mix** solution. Incubate for 30 min in a humidity chamber.
18) Rinse the excess with PBS, PBS Tween, water, and let dry.
19) Analyze.

Observations:

9.5 Cytometer sample protocol

Run Sheet for Cytometer Sample Testing

Operator: Trial:

Date:

Location:

- Laminated chamber (if toxic/pathogenic), PDMS room, basement room #020
- Biolab, basement room #011

Material / Reagents / Equipment:

- Magnetic separator
- Automatic mixer
- Magnetic Particles solution (MP; concentration:) in PBS
- Sample (concentration:)
- Sample's antibodies (AB; concentration:) in PBS
- BSA 5% solution in PBS
- PBS solution
- PBS Tween 20 0.02% solution
- Paper towel for cleaning
- Three Eppendorf tubes
- Isopropyl alcohol (IPA) for cleaning
- Distilled water for cleaning
- Gloves

Process Time: 2h30

Process:	**Time:**
Location: Table or laminated chamber	**Operator:**

1) Place 10 µL MP to a new Eppendorf. Wash. Remove supernatant.
2) Add 10 µL PBS. Spin-down.
3) Add 5 µL of the previous solution to a two new Eppendorf, +50 µL PBS.
4) To one of the previous Eppendorf (nSample), simply add 10 µL PBS. Re-suspend & agitate for 1 hour.
5) To the other Eppendorf (pSample), add 10 µL AB. Re-suspend & agitate for 1 hour.
6) Wash, remove supernatant, and add 50 µL 5% BSA. Incubate for 40 minutes.
7) Ready the solution of spores (100 µL)
8) Wash, remove supernatant, and add 10 µL of spores to each of the Samples + 40 µL PBS. Agitate for 30 minutes.
9) Add 50 µL PBS. Analyze the amount desired.

Observations: